




ORIGINAL ARTICLE

The crane fly glycosylated triketide δ -lactone cornicinine elicits akinete differentiation of the cyanobiont in aquatic *Azolla* fern symbioses

Erbil Güngör¹  | Jérôme Savary² | Kelvin Adema¹ | Laura W. Dijkhuizen¹  | Jens Keilwagen³ | Axel Himmelbach⁴ | Martin Mascher⁴  | Nils Koppers⁵ | Andrea Bräutigam⁵ | Charles Van Hove⁶ | Olivier Riant² | Sandra Nierzwicki-Bauer⁷ | Henriette Schluepmann¹ 

¹Department of Biology, Utrecht University, Utrecht, The Netherlands

²Institute of Condensed Matter and Nanosciences, Université Catholique de Louvain, Louvain-la-Neuve, Belgium

³Julius Kühn-Institute, Quedlinburg, Germany

⁴Leibniz-Institute of Plant Genetics and Crop Plant Research (IPK), Seeland, Germany

⁵Computational Biology, Center for Biotechnology and Faculty of Biology, Bielefeld University, Bielefeld, Germany

⁶Emeritus Professor from the Université Catholique de Louvain, Louvain-la-Neuve, Belgium

⁷Darrin Fresh Water Institute, Rensselaer Polytechnic Institute, Troy, New York, USA

Correspondence

Henriette Schluepmann, Department of Biology, Utrecht University, Padualaan 8, 3584 CH Utrecht, The Netherlands.
Email: h.schlupmann@uu.nl

Present addresses

Kelvin Adema, Laboratory of Molecular Biology, Wageningen University & Research, Wageningen, The Netherlands.

Nils Koppers, Core Facility Genomics, Medical Faculty of Muenster, University of Muenster, Muenster, Germany.

Funding information

Nederlandse Organisatie voor Wetenschappelijk Onderzoek; Aard- en Levenswetenschappen, Nederlandse Organisatie voor Wetenschappelijk Onderzoek

Abstract

The restriction of plant-symbiont dinitrogen fixation by an insect semiochemical had not been previously described. Here we report on a glycosylated triketide δ -lactone from *Nephrotoma cornicina* crane flies, cornicinine, that causes chlorosis in the floating-fern symbioses from the genus *Azolla*. Only the glycosylated trans-A form of chemically synthesized cornicinine was active: 500 nM cornicinine in the growth medium turned all cyanobacterial filaments from *Nostoc azollae* inside the host leaf-cavities into akinetes typically secreting CTB-bacteriocins. Cornicinine further inhibited akinete germination in *Azolla* sporelings, precluding re-establishment of the symbiosis during sexual reproduction. It did not impact development of the plant *Arabidopsis thaliana* or several free-living cyanobacteria from the genera *Anabaena* or *Nostoc* but affected the fern host without cyanobiont. Fern-host mRNA sequencing from isolated leaf cavities confirmed high NH_4 -assimilation and proanthocyanidin biosynthesis in this trichome-rich tissue. After cornicinine treatment, it revealed activation of Cullin-RING ubiquitin-ligase-pathways, known to mediate metabolite signaling and plant elicitation consistent with the chlorosis phenotype, and increased JA-oxidase, sulfate transport and exosome formation. The work begins to uncover molecular mechanisms of cyanobiont differentiation in a seed-free plant symbiosis

This is an open access article under the terms of the [Creative Commons Attribution](https://creativecommons.org/licenses/by/4.0/) License, which permits use, distribution and reproduction in any medium, provided the original work is properly cited.

© 2024 The Authors. *Plant, Cell & Environment* published by John Wiley & Sons Ltd.

important for wetland ecology or circular crop-production today, that once caused massive CO₂ draw-down during the Eocene geological past.

KEYWORDS

2-oxoglutarate-dependent dioxygenase evolution, *Azolla* symbioses, cyanobacteria cell differentiation, glycosylated triketide δ -lactone, jasmonic acid oxidase, N₂-fixation, *Nephrotoma cornicina*, *Nostoc azollae*, plant elicitation

1 | INTRODUCTION

Azolla is a genus of highly productive aquatic ferns in symbiosis with the N₂-fixing filamentous cyanobacteria *Nostoc azollae* (Nostoc). Nostoc is maintained in the fern meristems and specialized leaf cavities where it fixes enough N₂ to sustain the astonishing growth rates of the symbiosis (Brouwer et al., 2017). The ferns' massive depositions in Arctic sediments dating from the Eocene suggest that *Azolla* ferns (*Azolla*) may have caused climate cooling (Brinkhuis et al., 2006). In the past they were deployed as a biofertilizer, today they have great potential for the restauration of subsiding wetlands or for the circular use of mineral nutrients in sustainable agriculture to produce high-protein feed (Schluepmann et al., 2022). Despite this and the similar importance of symbioses with filamentous cyanobacteria such as mosses (Stuart et al., 2020), the mechanisms maintaining the coordinated development of cyanobiont and host are poorly understood. Here we learn from nature how a chemical from the crane fly, *Nephrotoma cornicina* interferes with these mechanisms at nanomolar concentrations.

Morphological observations have associated secretory trichomes (ST) with symbiosis maintenance in the shoot apical meristems, upper leaf lobes and inside the sporocarps (Calvert et al., 1985; Zheng et al., 2008). At the shoot tips, the cabbage-like crop of leaves tightly conceals the important shoot-apical Nostoc colony (SANC) and large ST. The small and likely motile SANC filaments inoculate newly forming leaf initials and sporocarps, for vertical transfer of Nostoc to the next generation (Dijkhuizen et al., 2021). Inside the cavities of the upper leaf lobes, mature N₂-fixing Nostoc filaments are typically found along with a variety of ST. Under the indusium cap of the megasporocarp, ST are found along with Nostoc akinetes.

Lipids and flavonoids from the fern host are known to control cyanobiont differentiation. Nostoc from the SANC was proposed to differentiate into motile hormogonia by hormogonia-inducing factors (HIF) secreted by the shoot apical ST, after which the hormogonia are attracted to the ST inside developing leaf cavities (Cohen et al., 2002). Diacylglycerols acting as HIF on *Nostoc* species have been isolated from the symbiotic coralloid roots of *Cycas revoluta* (Hashidoko et al., 2019). Attraction of Nostoc filaments to *Azolla* ST has been hypothesized (Cohen et al., 2002). Once inside the leaf cavity hormogonia differentiate into filaments with heterocysts that actively fix N₂. Therefore, the leaf-cavity ST were proposed to secrete hormogonia suppressing factors (HSF) to keep Nostoc in this state. Glycosylated flavonoids such as 3-deoxyanthocyanins isolated from *Azolla* and naringin have been shown to act as HSF on *Nostoc punctiforme* (Cohen et al., 2002). In addition,

nostopeptolides secreted by *N. punctiforme* itself act as HSF as shown by a restored phenotype when a polyketide synthase (PKS) knock-out mutant, which lacks nostopeptolides and differentiates into hormogonia by default, was supplemented with nostopeptolides (Liaimer et al., 2015). At a low concentration, nostopeptolides also acted as chemoattractant. Interestingly, when in symbiosis with the plant hosts *Gunnera manicata* or *Blasia pusilla*, nostopeptolide production by *N. punctiforme* was down-regulated. Plant exudates, therefore, do influence nostopeptolide production and herewith regulate the movements and state of the cyanobiont.

Sporocarp initials (SI) of *Azolla* also have ST that presumably attract Nostoc and thus mediate vertical transfer of Nostoc in the life cycle of the host (Perkins & Peters, 2006; Zheng et al., 2008). In SI developing into microsporocarps, the Nostoc are not entering the microsporangia and are thus eventually lost. In contrast, the megasporocarps develop a protective indusium cap under which the Nostoc accumulate and then differentiate into akinete resting stages. Akinete inducing factors may not be required for this process because filamentous cyanobacteria are known to differentiate into akinetes when resources are limited (Zheng et al., 2013). Akinetes in the megasporocarp may be limited in nutrients and light, based on their isolation from the nutritious megaspore and the light-absorbing dark indusium cap. When an *Azolla* sporeling germinates on the tiny gametophyte formed inside the megasporocarp, it pushes towards the indusium cap. When it displaces the cap and grows through the indusium chamber it develops ST which are thought to reestablish the SANC (Dunham & Fowler, 1987; Peters & Perkins, 2006).

The natural environment constitutes the biggest available nonrandom chemical library screen to research what maintains the symbiotic interaction. Insects are the largest group in the animal kingdom and they excel at recruiting microbial symbionts with special metabolic capabilities to fill an enormous range of niches (Feldhaar, 2011). Examples of processes insect symbionts help with are digestion, detoxification and antibiotic production. Insect extracts are, therefore, a promising source to discover novel chemicals (van Moll et al., 2021). A common insect found in wetlands where *Azolla filiculoides* also thrives in the Netherlands is the crane fly *N. cornicina* (de Jong et al., 2021). These crane flies possibly spend most of their life cycle as larvae in water-drenched soil feeding on detritus while the adults only appear for sexual reproduction in midsummer. Corpses of *N. cornicina* crane flies caused chlorotic spots in *Azolla* mats (Figure 1a). To reveal the compounds causing this phenomenon, some 10,000 adult crane flies were collected, boiled in water, and the

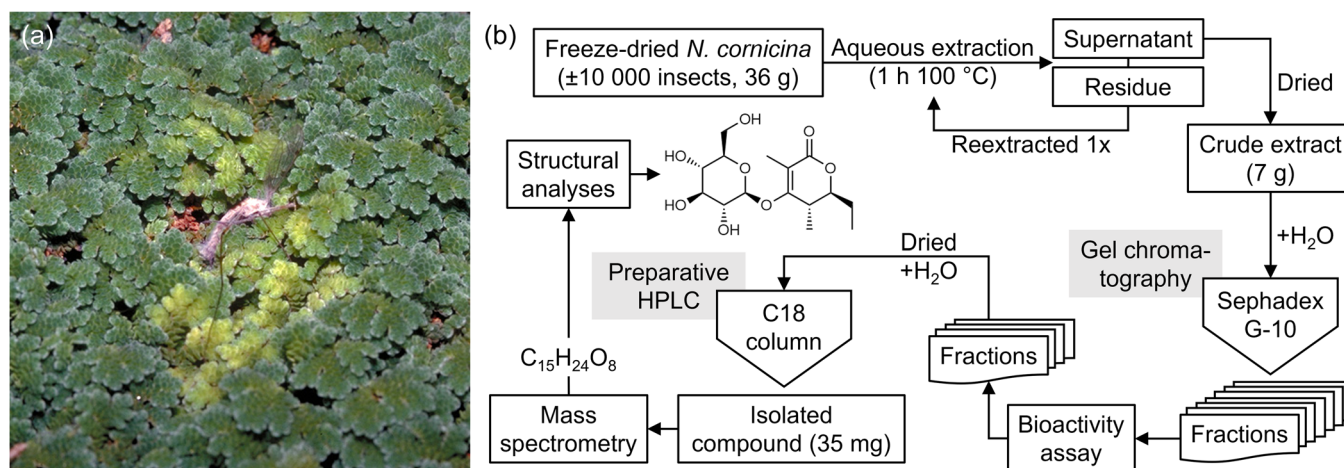


FIGURE 1 *Nephrotoma cornicina* induced chlorosis in *A. filiculoides* mats and isolation procedure of cornicine. (a) Typical chlorotic halo in *Azolla* mats induced by an *N. cornicina* corpse. (b) Overview of the procedure used to isolate, bioassay and identify cornicine. Dry *N. cornicina* (36 g) were extracted in water, then freeze-dried yielding 7 g of dry powder. The powder was redissolved and fractionated on a Sephadex G-10 column. Fractions were assayed for bioactivity and the bioactive fractions, with a shared maximum absorption at 254 nm, were pooled. The absorption peak was used to isolate 35 mg of a pure compound by preparative HPLC. Structure elucidation by way of mass spectrometry and NMR experiments revealed a novel glycosylated triketide δ -lactone, with likely trans diastereomeric configuration, named cornicine.

crude extract thus obtained fractionated; the fractions were tested for bioactivity (Figure 1b). The bioactive fractions eluted consecutively, they were thus pooled and contained a single compound with maximum absorption at 254 nm, accounting for $\pm 0.1\%$ DW of the crane fly biomass. Mass spectrometry and structural analyses characterized a novel glycosylated triketide δ -lactone, named cornicine, which was identified as the candidate molecule turning *Azolla* chlorotic (Mathieu et al., 2005). The relative activity of cornicine stereoisomers was not clarified.

Here we examined the specific occurrence of cornicine in insects from the genus *Nephrotoma*. We then tested chemically synthesized cornicine stereoisomers for activity on several *Azolla* species, *Arabidopsis thaliana* and free-living *Anabaena* or *Nostoc* species. To examine the effect of cornicine on the symbiosis physiology, dual RNA from whole symbioses and mRNA from isolated fern host leaf-cavities were sequenced. Given the akinete-like morphology of the *Nostoc* symbiont inside the cornicine-treated *Azolla* symbioses, the dual RNA sequencing profiles from cornicine-treated ferns were compared to those from megasporocarps where *bona fide* akinetes are formed. The profiles of fern transcripts from isolated leaf cavities that were obtained by ranking genes according to read counts were, firstly, validated against known activities in cells lining the leaf cavities and, secondly, evaluated for the effects of cornicine.

2 | MATERIALS AND METHODS

2.1 | *Azolla* strains and growth conditions

The four *Azolla* species used in this study were *A. filiculoides* (Li et al., 2018), *Azolla pinnata* originating from the Botanical Gardens of Antwerp (Belgium), an *Azolla* species from the Anzali lagoon (Iran)

which was phylogenetically analyzed but could not be assigned to any of the described *Azolla* species (Dijkhuizen et al., 2021) and an unknown *Azolla* species collected from the Botanical Gardens of Bordeaux (France). Adult *Azolla* sporophytes were grown in modified IRRI-medium as previously described (Brouwer et al., 2017) with a 16 h light period ($100 \mu\text{mol m}^{-2} \text{s}^{-1}$) at 21°C .

2.2 | Preparation of *Azolla* spores for germination experiments

Spores for germination experiments were harvested in fall 2019 from mature mats of *A. filiculoides* by giving the plants a pressurized shower through a set of sieves (mesh sizes: 1000, 500 and $200 \mu\text{m}$). Harvested spores were stored embedded in sludgy root debris at 4°C . Shortly before use the sludge was diluted with water and agitated in a wide container. Distinguishably yellow-colored clumps of megasporocarps, held together by the glochidia of the massulae, could then be hand-picked from the shallow water and used.

2.3 | *N. cornicina*, isolation, bioassay and structural analyses of cornicine

The thousands *N. cornicina* (Linnaeus, 1758) (Tipulidae, Diptera) used for the initial identification of cornicine were collected in the surroundings of Louvain-la-Neuve (Belgium). Entomologists from various parts of the world kindly provided material from their country (see Figure 1, Figure S1C). Bioassay, isolation procedure and structural elucidation of cornicine has been described in patent EP1697392A1 (Mathieu et al., 2005). Briefly, bioassays on fern fronds in liquid medium were carried out with $4 \mu\text{g mL}^{-1}$ of dry *N. cornicina* powder, or fractions

thereof. For structural analyses, aqueous extract from *N. cornicina* (about 10 000 adults) was fractioned on a Sephadex G-10 column and assayed for bioactivity. 35 mg of a pure compound could be isolated from the bioactive fractions with preparative high performance liquid chromatography (HPLC) on a C18 column. APCI/HREI mass spectrometry revealed the compound had a sugar moiety and the mass of the isolated aglycone corresponded to $C_9H_{14}O_3$. nuclear magnetic resonance spectroscopy (NMR) experiments (INADEQUATE, HSQC, HMBC, COSY, ROESY and NOE) followed by structural analyses revealed a novel glycosylated triketide δ -lactone which was called cornicinine ($C_{15}H_{24}O_8$). Cornicinine could have three possible isomeric configurations (cis, trans-A and trans-B) but the trans-configuration fitted best with the NMR-data (Mathieu et al., 2005).

2.4 | Chemical synthesis and characterization of cornicinine stereoisomers and their aglycone precursors is described in Method S1 and Figure S2

2.5 | Cornicinine assays on *Azolla*

The synthesized compounds were tested by putting ± 3 mm *Azolla* shoot tips in 1.5 mL IRRI-medium in a 24-well plate and supplementing 500 nM of each compound dissolved in water. 1 mM KNO_3 was added to the IRRI-medium to test the effect of nitrate and cornicinine together on *Azolla*. To test the effect of cornicinine on germinating sporelings, clumps of ± 50 megasporocarps were inoculated in 1.5 mL water supplemented with 500 nM cornicinine. Buoyant sporelings surfaced after 10 days and were transferred to fresh IRRI-medium with 500 nM cornicinine during further development.

2.6 | Cornicinine assays on *Arabidopsis thaliana* and free-living filamentous Cyanobacteria

A. thaliana Col-0 seeds were sterilized for 3 h by chlorine gas vapor and sown on $\frac{1}{2}$ MS medium including vitamins pH 5.8 with 0.8% agarose and 500 nM cornicinine. The seeds were stratified for 2 days at 4°C and moved to a 16 h light period ($100 \mu\text{mol m}^{-2} \text{s}^{-1}$) at 21°C. *Anabaena* sp. PCC 7210 was inoculated in BG-11₀ medium with 500 nM cornicinine and grown under constant light ($25 \mu\text{mol m}^{-2} \text{s}^{-1}$) at 30°C. Growth was tracked by measuring OD₆₆₅ of methanolic extracts and the formula: chlorophyll (mg/mL) = $13.45 \cdot \text{OD}_{665} \cdot \text{dilution factor}$. Akinete induction was tested on free-living cyanobacteria donated by Dr. Henk Bolhuis (NIOZ, Texel, The Netherlands), incubating them in BG-11₀ medium in the presence of 500 nM cornicinine.

2.7 | Microscopy

N. azollae was visualized by squeezing the outermost tip of an *Azolla* branch between two glass slides with a drop of demineralized water.

A Zeiss Axio Zoom.V16 microscope with a Zeiss Axiocam 506 color camera, Zeiss CL 9000 LED lights and a Zeiss HXP 200 C fluorescence lamp with standard Zeiss RFP filter set 63HE (excitation 572 nm, emission 629 nm) was used for imaging. Images were Z-stacked with Helicon Focus 7 software in default settings (depth map, radius 8, smoothing 4). The same set-up was also used to image sporelings, leaf cavities and free-living filamentous cyanobacteria.

2.8 | Sequencing, assembly and annotation of the *A. filiculoides* genome version 2 (Afi_v2)

To improve the first genome assembly (4666 scaffolds; Azfivs1), *A. filiculoides* PacBio RSII sequencing data from Li et al., 2018 was processed anew. PacBio RSII reads were corrected, trimmed and assembled with Canu (Koren et al., 2017) in 4632 scaffolds. The assembly was then polished with Quiver (Chin et al., 2013) and Pilon (Walker et al., 2014). To reduce fragmentation, we implemented optical mapping. We grew *A. filiculoides* without cyanobacteria under sterile conditions, extracted nuclei as described in Dijkhuizen et al., 2018, extracted high molecular weight DNA (above 150 kb) and ran Bionano Genomics chips once this DNA was labelled as per the manufacturer's instructions. With the optical maps, the new *A. filiculoides* genome assembly was reorganized into 4422 scaffolds.

To further reduce fragmentation, we resorted to incorporating tethered chromosome conformation capture sequencing (TCC). The TCC library was prepared essentially as described previously (Himmelbach et al., 2018) from 2.4 g of the same fresh plant material as for the optical mapping. The library was sequenced using a HiSeq. 2500 (Illumina Inc.). TCC data was then used to correct and improve the optically mapped assembly (Mascher et al., 2017). The final Afi_v2 assembly contains 3585 scaffolds totaling 579 Mbp with an N50 of 4 Mbp and L50 of 35. Afi_v2 is shorter than the 622.6 Mb, but its N50 is much improved over the N50 of 965 kb, compared to the first assembly (Li et al., 2018).

To improve on the first *A. filiculoides* annotation, we included existing unstranded RNA sequencing data (Brouwer et al., 2017; de Vries et al., 2016) and more recent stranded and dual RNA sequencing data (Dijkhuizen et al., 2021). RNA-sequencing data were mapped to the Afi_v2 assembly with STAR (Dobin et al., 2013) and gene predictions were made with GeMoMa (Keilwagen et al., 2019). We used a gene predominant splice form of the gene models predicted by GeMoMa for analyses of Single Copy Orthologs with the viridiplantae_odb10 database (BUSCO v5.6.1, Manni et al., 2021) and read counting. BUSCO revealed that the Afi_v2-gene set was 96.2% complete with 10.6% duplicated single copy orthologs (C:96.2% [S:85.6%, D:10.6%], F:0.5%, M:3.3%, $n = 425$; Figure S3, genes). For comparison, the Azfivs1 gene set was 81.7% complete with 7.3% duplicated single copy orthologs (C:81.7% [S:74.4%, D:7.3%], F:9.6%, M:8.7%, $n = 425$). Our searches for 2-oxoglutarate-dependent dioxygenase enzymes resulted in 22 gene models predicted for Azfivs1 but 29 for Afi_v2.

2.9 | Leaf-pocket isolations from *A. filiculoides* and sequencing of their polyA-enriched RNA

Leaf pockets were isolated from *A. filiculoides* as described before with slight modifications (Peters et al., 1978; Uheda, 1986). Briefly, about 3 g of *Azolla* was prepared by removing roots and rinsing with 0.1% v/v Triton X-100 and demineralized water. Cleaned sporophytes were submerged in enzyme solution (0.5 M mannitol with 2% w/v cellulase, 1% w/v macerozyme, 0.1% w/v pectolyase, 1% w/v PVP and 10 mM DTT) and vacuum infiltrated for 10 min at 0.6 bar before incubation for 19 h at 30°C with gentle agitation. Leaf pockets were released by washing the digested sporophytes with 0.5 M mannitol through a mesh. The flow-through was left to settle for 10–30 min after which the sunk leaf cavities were manually collected and washed in PBS before snap freezing.

The experiment was set up so as generate three biological replicates to compare RNA extracted from sporophytes with that of isolated leaf pockets, and to compare RNA in leaf pockets isolated from ferns grown with and without 500 nM cornicinine for 6 days. Care was taken to snap-freeze the ferns and isolated leaf cavities 2–3 h into the light cycle of the diel rhythm. Total RNA from ± 80 isolated leaf cavities was extracted with the RNeasy Micro Kit (Qiagen). Total RNA from 50 mg FW sporophytes was isolated with the Spectrum Plant Total RNA Kit (Sigma-Aldrich) applying protocol B. Total RNA was treated with DNase I (Thermo Fisher Scientific) for 1 h at 37°C after which the reaction was stopped by adding two mM EDTA and incubation for 10 min at 65°C. The reactions were cleaned with the RNeasy MinElute Cleanup Kit (Qiagen). Poly-A tail enriched cDNA libraries were prepared using the SMART-Seq HT Kit (Takara Bio), quality checked using the TapeStation DNA ScreenTape (Agilent Technologies) then sequenced on a half lane NovaSeq. 6000 using the paired-end 2 × 50 cycle chemistry (Illumina). Data is deposited under accession PRJEB60092.

2.10 | Dual RNA sequencing to compare akinete induction in sporocarps and in sporophytes after cornicinine

To compare sporophyte profiles with those from micro- and megasporocarps, *A. filiculoides* ferns were grown on light with a far-red component to induce sporulation as described in Dijkhuizen et al., 2021. Micro- and megasporocarps were manually picked from the sporulating ferns during a period of 2 h, 2 h into the light period, snap frozen along with the sporophytes collected 2 h into the light period. Material was sampled from independent cultures so as to obtain three independent biological replicates. Sporophytes were grown with a far-red-light component as above and three replicate cultures were treated each for 6 days (C6) and overnight (Co/n) with cornicinine (500 nM), whilst another three were without (cornicinine control, CC), biological replicate sampling was 2 h into the light period. RNA was extracted, then libraries synthesized and dual RNA sequenced as described in Dijkhuizen et al. (2021). Data from these experiments is deposited under accession PRJEB60372.

2.11 | Analysis of the differential mRNA accumulation in leaf-pocket preparations

After demultiplexing, quality filtering and trimming of the sequencing primers away from the reads, approximatively paired reads per sample were aligned using the STAR aligner with default settings to the concatenated genome assemblies of the *A. filiculoides* nucleus Afi_v2, its chloroplast and *N. azollae*, extracting read counts for Afi_v2 only.

Read counts for the Afi_v2 gene models (predominant splice versions only) were normalized as reads per million, except for leaf-pocket profiling. For the later, normalization was to the sum of counts from the 1100 most-expressed genes in each sample because of the large difference in the sensitivity of the assay when comparing sporophytes with leaf cavity. For statistical analyses of differential gene expression with DESeq. 2 (Love et al., 2014), the genes with no expression in all leaf-pocket samples were removed from the analyses. In addition, the sample leaf pocket 2 from sporophytes grown on cornicinine was removed from the analysis because of its large contamination with sporophyte RNA.

2.12 | Phylogenetic analysis of cyanobacterial tandem bacteriocin (CTB) family bacteriocins and 2-oxoglutarate-dependent dioxygenases (2OGD)

CTB family bacteriocin protein sequences were extracted from the NCBI NF038167.1 filtering on species with diverse habitat, aligned with MAFFT-einsi (Katoh et al., 2019), then the phylogeny computed with IQ-tree (Nguyen et al., 2015). Protein sequences of 2OGD in the two *A. filiculoides* genome assemblies and annotations were identified by local BLAST using as query 2OGD automatically annotated by Mercator (Lohse et al., 2014). These were compared to functionally characterized DOXC-genes from seed plants (Kawai et al., 2014) and bryophytes (Li et al., 2020) then integrated in the corresponding 1kp orthogroup (Ka-Shu Wong et al., 2019). The orthogroup was sub-sampled selecting specific species and sequences were aligned with MAFFT-einsi, and then trimmed using trimAL (Capella-Gutiérrez et al., 2009). The phylogeny was computed with IQ-tree with 200 bootstraps. Bootstrap support was calculated as transfer bootstraps (Lemoine et al., 2018). A subset of the phylogeny containing jasmonic acid oxidase (JOX), ANS and FLS clades was recomputed similarly. Both trees were annotated in iTOL (Letunic & Bork, 2019) and Inkscape. Code and data for the phylogeny are available at https://github.com/lauralwd/2OGD_phylogeny.

2.12.1 | Accessions

PRJEB60092 polyA-enriched RNAseq for cornicinine treated *A. filiculoides* leaf-pocket reads, PRJEB60372 rRNA depleted dual RNAseq for cornicinine treated, and reproductive structures of *A. filiculoides*. PRJEB60371 for the Afivs2 *A. filiculoides* assembly.

3 | RESULTS

3.1 | *N. cornicina* collected from around the world cause chlorosis

Corpses of the *N. cornicina* observed on the canopy of *Azolla* at the Belgium site of initial discovery were often infected with fungi (Figure 1a, Figure S1A). Microbes including fungi from the surrounding environment thriving on just about any insect biomass may therefore have been the source of the active substance. Different species of *Nephrotoma* were tested for activity including *N. aculeata*, *appendiculata*, *crocata*, *flavescens*, *flavipalpis*, *guestfalica*, *pratensis*, *quadrifaria*, *scalaris*, *scurra* and *submaculosa*. None of the adults from these species proved to induce chlorosis; generalist microbes on corpses from insects sharing the wetland habitat were thus not involved (Figure S1B). To exclude abiotic and biotic effects of the environment, we tested *N. cornicina* individuals from Ottawa (Canada), Lucas Marsh (United Kingdom), Köyceğiz (Turkey), Segezha, Vyatka, Krasnoyarsk, Irkutsk and Sakhalin (Russia), and Kyushu (Japan), all of which displayed activity (Figure S1C). We thus concluded that the compound is not synthesized by microbes recruited from the environment but is systematically associated with *N. cornicina*.

3.2 | Only the trans-A diastereoisomer of cornicinine turns all tested *Azolla* species chlorotic; its aglycone does not

To verify the identity and activity of cornicinine purified from *N. cornicina*, two stereoisomers were synthesized chemically as described in Methods S1 based on Hinterding et al., 2001: the trans-A (with the R,R-lactone) and trans-B (with the S,S-lactone) (Figure 2a). The aglycone lactones were synthesized from the commercially available propionyl oxazolidinone stereoisomeric precursors, then glucose was added with acetylated hydroxyl groups to direct condensation reactions, and resulting acetylated intermediates were deacetylated (Figure 2a, Figure S2). Key to the synthesis of the aglycone lactone, which was achieved in three steps, were the conditions to generate the Evans anti-adduct and its subsequent high-yield (71%) intramolecular lactonization in an excess of KHMDS at -78°C (Figure S2A). Overall, the yields for aglycone lactone synthesis were similar for the stereoisomers: 37% and 34%, respectively, for cornicinine and its diastereoisomer (Figure S2B-C). The O-glycosylation (68% yield) and de-acetylation (81% yield) had higher combined yields.

For both stereoisomeric forms, the aglycone, acetylated synthesis intermediate and cornicinine were then supplemented, at a concentration of 500 nM, to growth medium with shoot tips of four different *Azolla* species representing both sections of the *Azolla* genus: *Azolla* and *Rhizosperma*. After 25 days, the ferns supplemented with trans-A cornicinine were chlorotic but not those with trans-B cornicinine (Figure 2b). The first signs of yellowing and growth retardation were already visible after 6 days and gradually increased over time (Figure S4). The aglycone did not cause chlorosis, proving that glycosylation is

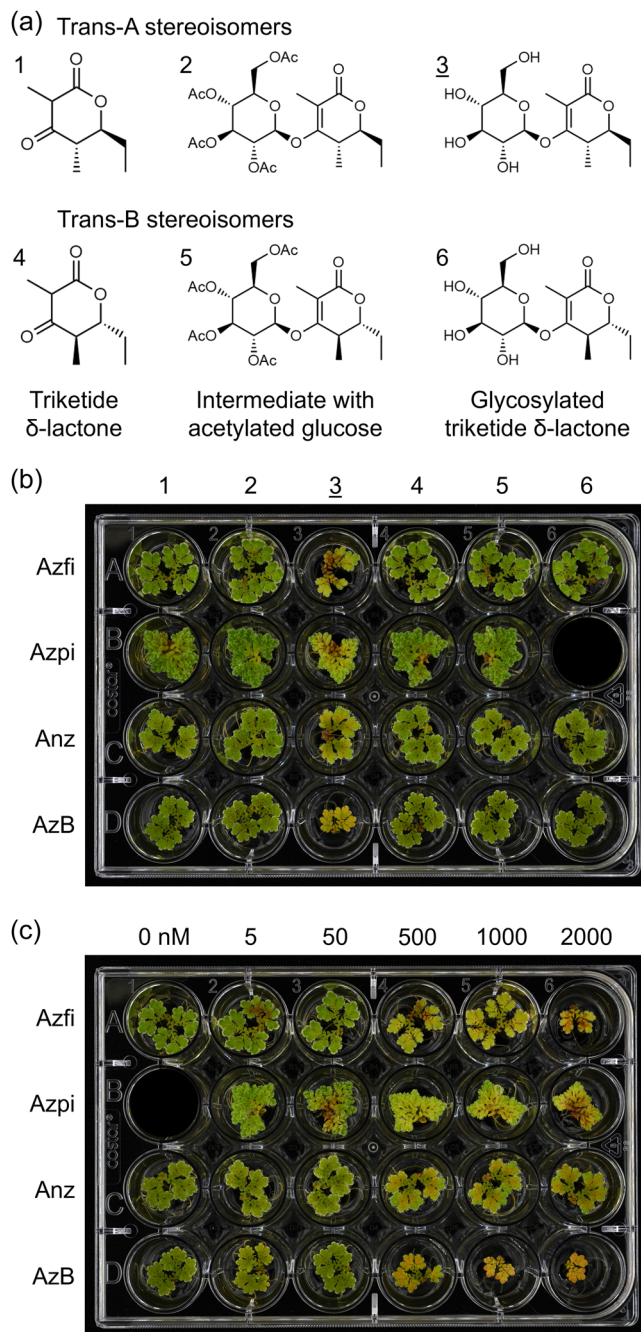


FIGURE 2 Effect of synthetic trans-stereoisomers of cornicinine, their aglycones and acetylated precursors on four *Azolla* species. (a) Overview of the compounds chemically synthesized in trans-A and trans-B configuration, respectively: compound 1 and 4 are the aglycones, compound 2 and 5 are the synthesis intermediates with an acetylated glucose and compound 3 and 6 are cornicinine and its diastereoisomer. (b) fern fronds from *Azolla* species after 25 days on 500 nM of the compounds from (a). (c) fern fronds from *Azolla* species after 25 days on a concentration gradient from 0 to 2000 nM of the bioactive trans-A diastereoisomer cornicinine, compound 3 in (b). Azfi: *A. filiculoides*; Azpi: *A. pinnata*; Anz: *Azolla* species from Anzali (Iran); AzB: *Azolla* species from Bordeaux (France). [Color figure can be viewed at [wileyonlinelibrary.com](https://onlinelibrary.wiley.com/doi/10.1111/pcel.14907)]

essential for the bioactivity of trans-A cornicinine (from now on referred to as cornicinine). The acetylated compounds also had no activity.

When testing cornicinine concentrations ranging from 5 nM to 2000 nM, 500 nM cornicinine generally sufficed to cause chlorosis in all species tested (Figure 2c). *A. filiculoides* and *A. pinnata* turned yellow and stopped growing gradually over time when on 500–2000 nM cornicinine (Figure 2c, Figure S5). *Azolla* sp. Bordeaux was the most sensitive with severe growth retardation at 1000 nM cornicinine and above. *Azolla* sp. Anzali was affected the least with similar growth rate and phenotype at 500–2000 nM cornicinine. Both, the species from Bordeaux and Anzali started turning red consistent with 3-deoxyanthocyanin accumulation after 17 days (Figure S5). The chlorosis combined with growth retardation made us wonder about the physiological state of the cyanobacterial symbiont.

3.3 | Cornicinine induces the coordinate differentiation of *N. azollae* filaments from the leaf cavities into akinete-like cells (ALC) within 6 days

We visualized Nostoc by crushing shoot tips between two glass slides for microscopy after 12 days growth with 500 nM synthetic compound. Cornicinine-treated *A. filiculoides* fern fronds did not have the heterocyst-rich Nostoc filaments characteristic of leaf cavities (Figure 3a). Instead, single, larger cells with cyanophycin granules accumulated that resembled the akinetes found under the indusium cap of the megasporocarp (Figure S6). The cornicinine-induced akinetes had a more elongated shape than those typical of the indusium and we therefore called them ALC. The shapes of the ALC of the four tested *Azolla* species looked surprisingly different (Figure 3b). The ALC of *A. filiculoides* mostly contained two to five cyanophycin granules while the ALC of *A. pinnata* were smaller and did not seem to contain any granules. The ALC of the *Azolla* species from Anzali and Bordeaux were larger, sometimes rhombus shaped, and contained five to ten granules.

The trans-B stereoisomer and aglycone of cornicinine neither induced ALC, chlorosis nor growth retardation. Development of ALC thus had to be a result of cornicinine. We followed the development of ALC over time and with a range of concentrations. After 6 days on more than 1000 nM cornicinine, all Nostoc from *A. filiculoides* fern fronds were differentiated into ALC, while on 500 nM cornicinine isolated filaments were still present albeit with somewhat bloated vegetative cells (Figure S7). These bloated filaments eventually completely disassociated into ALC between Day 8 and 12. Fern fronds treated with ≤ 50 nM cornicinine still contained filaments even after 21 days indicating that a threshold concentration is required before ALC are formed (Figure S7).

The first signs of yellowing and growth retardation after 6 days on 500 nM cornicinine coincided with the first signs of ALC-induction. A slight delay persisted, however, between the complete disappearance of filaments to the extent that only isolated ALC remain (Day 12) and chlorosis with growth retardation (Day 17–21) (Figure S5, Figure S7). ALC unlikely fix N_2 , as this process is usually attributed to heterocysts fueled by the metabolism of vegetative cells in the intact Nostoc filament. The

ferns may have temporarily relied on internally stored nitrogen in the time between complete ALC-induction and yellowing. Consequently, chlorosis may be a result of nitrogen starvation.

3.4 | Cornicinine-induced chlorosis is not alleviated by nitrate supplied in the medium

A. pinnata, *A. filiculoides* and a strain of *A. filiculoides* devoid of Nostoc (Brouwer et al., 2017) were grown with(out) 500 nM cornicinine and 1 mM KNO_3 . After 17 days, *A. pinnata* growth inhibition by cornicinine was suppressed by nitrate, but the chlorosis caused by cornicinine remained (Figure 4a, Figure S8). Nitrate neither suppressed the growth inhibition nor the chlorosis of *A. filiculoides* on cornicinine regardless of the presence of the cyanobacteria. We conclude that chlorosis was caused by something else than solely the nitrogen deficiency resulting from complete differentiation of the Nostoc into ALC. We next wondered whether cornicinine affects plants or free-living cyanobacteria.

3.5 | Cornicinine did not affect the growth and differentiation of Arabidopsis seedlings or free-living filamentous cyanobacteria

Given the overall similarity of cornicinine to sugar disaccharides, we tested the germination and growth of Arabidopsis seedlings on medium containing 500 nM cornicinine with(out) 100 mM sucrose, or 100 mM sorbitol osmoticum control. Whilst the seedlings responded to the sucrose and osmoticum, the 500 nM cornicinine did not have visible effects on germination time, and root or shoot growth rates and habit under any of the conditions tested (data shown for seedlings without sugars in Figure S9A). Similarly, 500 nM cornicinine did not alter the growth rates of *Anabaena* PCC 7210 (Figure S9B); it also did not induce the differentiation into akinetes in strains of an *Anabaena* sp., *Nostoc spugimena* and *N. punctiforme* when tested in the nitrogen-free BG-11₀ medium (Figure S9C). Therefore, cornicinine interferes with mechanisms specific for the symbiosis.

3.6 | Cornicinine inhibits the germination of akinetes from the megasporocarp during sporeling germination

To test whether cornicinine would affect the dedifferentiation of *bona fide* akinetes and sporeling germination, clumps of *A. filiculoides* spores were germinated in demineralized water with (out) 500 nM cornicinine. After 10 days, the first green sporelings popped up to the water surface and were all inoculated with akinetes, suggesting that cornicinine did not interfere with germination of the fern host (Figure 4b). Some akinetes were enclosed by the first emerging leaf, but the majority were just attached to the outer surface of the sporeling (Figure 4b, T10). The

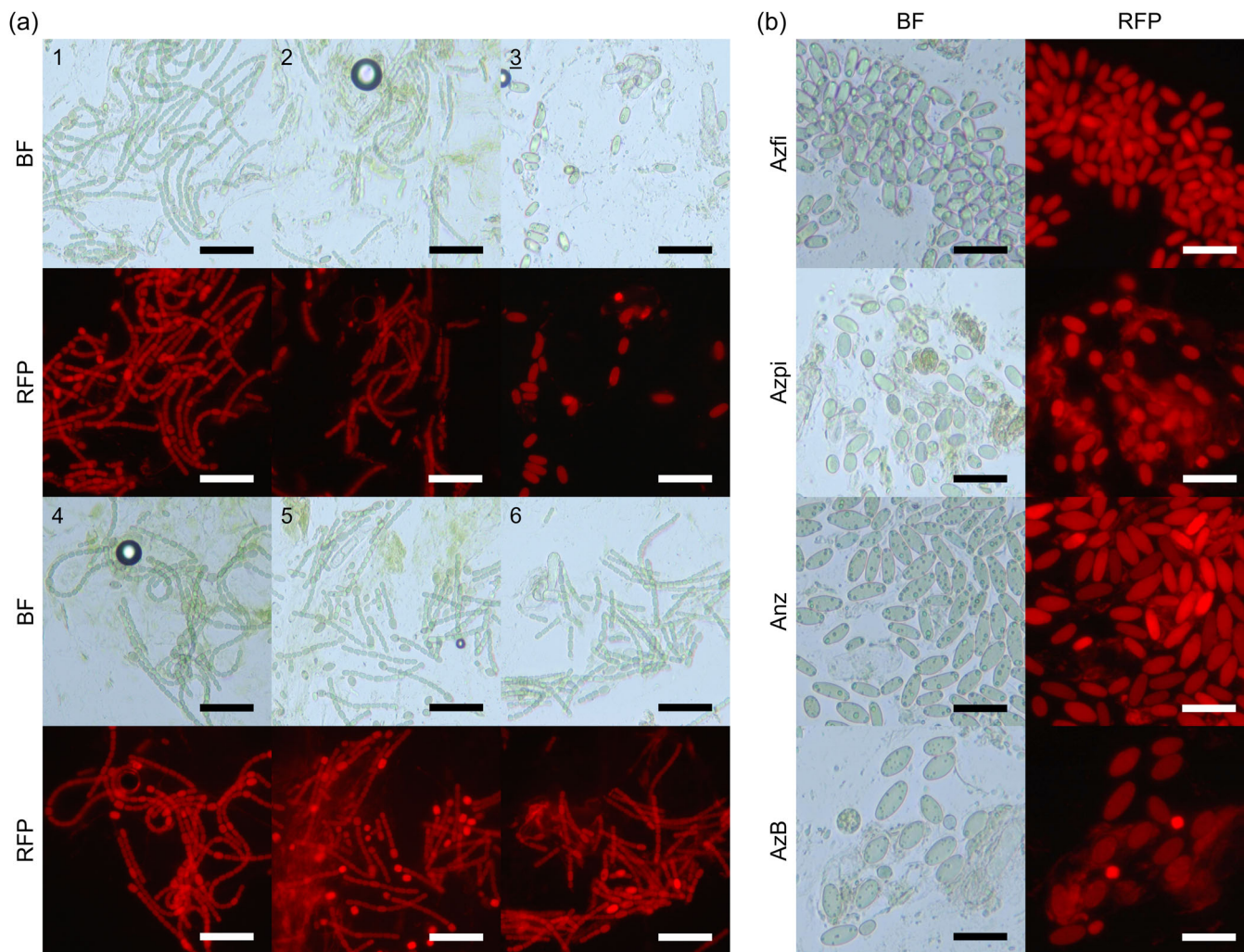


FIGURE 3 Effect of synthetic trans-stereoisomers of cornicinine, their aglycones and acetylated precursors on *Nostoc azollae* from four *Azolla* species. (a) *N. azollae* inside *A. filiculoides* after 12 days on 500 nM of the six compounds from Figure 2a, scale bars correspond to 50 µm. (b) Morphology of the akinete-like cells from four different *Azolla* species induced by 500 nM cornicinine after 12 days, scale bars correspond to 30 µm. The different *Azolla* species were as in Figure 2. BF, brightfield; RFP, fluorescence under the settings for red fluorescent protein (RFP). [Color figure can be viewed at [wileyonlinelibrary.com](https://onlinelibrary.wiley.com/doi/10.1111/pcse.14907)]

latter does not need motile *Nostoc* cells, it could have resulted from the sporeling growing through the indusium and engulfing the akinetes from under the indusium cap with its cup-shaped first leaf. After 12 days, the akinetes captured by sporelings not exposed to cornicinine proliferated into filaments whilst those from sporelings growing with cornicinine remained akinetes (Figure 4b, T12 -C vs T12 +C). After 21 days, the sporelings without cornicinine had already reached the four-leaf stage while those with cornicinine only reached the two-leaf stage (Figure S10). Cornicinine-treated sporelings did not exhibit the typical fluorescence under the RFP-settings compared to untreated sporelings: when crushed between two glass slides, however, akinetes were still found (Figure S10). The sporelings on cornicinine, therefore, failed to reestablish the symbiosis. Cornicinine inhibition of the germination of *bona fide* akinetes from *Nostoc* meant that it interferes with processes controlling the differentiation of the symbiont.

3.7 | Transcripts of the *Nostoc* CTB-bacteriocin cluster accumulate highly in akinetes

Dual RNA sequencing of sporophytes on cornicinine for 6 days versus without, and of megasporocarps versus sporophytes, yielded lists of differentially accumulating *Nostoc* transcripts when akinetes are induced (File S1, $\text{padj} < 0.1$): 140 of 232 upregulated *Nostoc* transcripts on cornicinine were also up in megasporocarps. Similarly, 62 of the downregulated *Nostoc* transcripts on cornicinine were also down in megasporocarps. The most upregulated *Nostoc* transcript cluster on cornicinine ($\log_2\text{FoldChange}$ 3.29–7.35) and in megasporocarps ($\log_2\text{FoldChange}$ 5.14–7.09) encoded five class II bacteriocins belonging to the CTB family at the same locus (AAZO_RS0345 to AAZO_RS0365, Figure 5a,b). The CTB operon additionally encoded a peptidase containing ABC transporter and the HlyD known to export, cleave and secrete the peptides. Phylogenetic analyses revealed that CTB bacteriocins from the

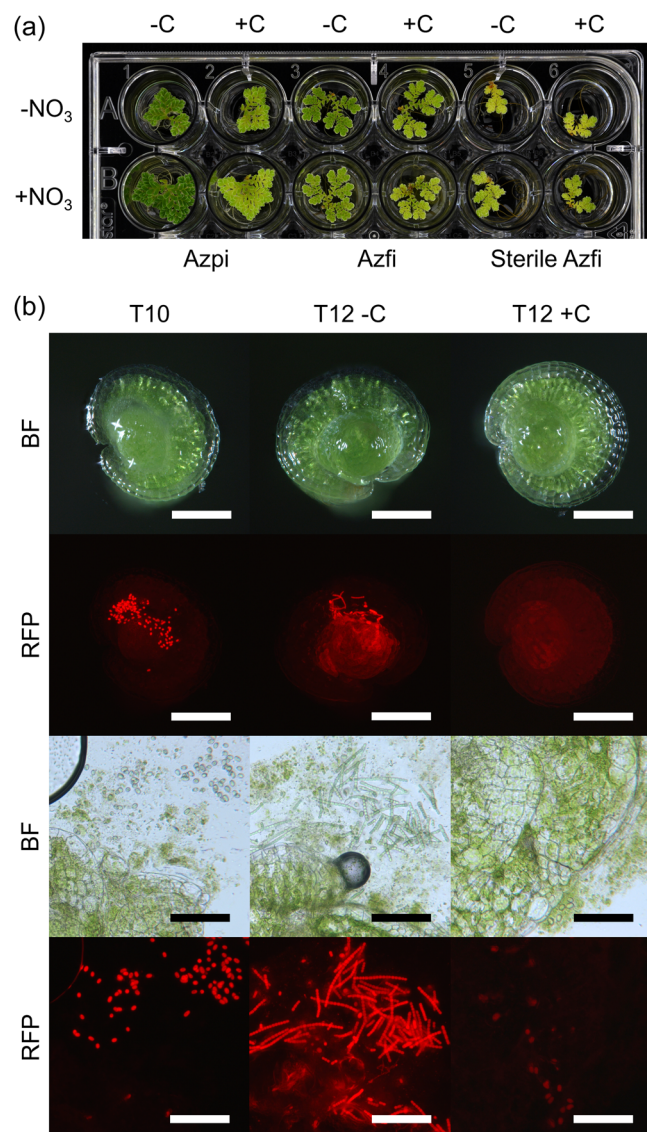


FIGURE 4 Effect of cornicinine when sporophytes grow on nitrate supplemented medium and during the reestablishment of the symbiosis when sporelings germinate. (a) *A. pinnata*, *A. filiculoides* and *A. filiculoides* devoid Nostoc after 17 days without (–C) and with 500 nM cornicinine (+C) and 1 mM KNO_3 ($\pm\text{NO}_3$). (b) Top: from left to right, *A. filiculoides* sporeling 10 days after germination, and sporelings 12 days after germination with(out) 500 nM cornicinine ($\pm\text{C}$). Bottom: the same sporelings crushed to expose *Nostoc azollae*. Images are representative for 15 individual sporelings imaged per condition. Scale bars on top and bottom, respectively, correspond to 200 and 100 μm . BF, brightfield; RFP, fluorescence under RFP settings. [Color figure can be viewed at wileyonlinelibrary.com]

N. azollae operon clustered with those encoded by other filamentous cyanobacteria, including symbionts in plants (hornworts, cycads and ferns), insects and lichen (Figure 5c). However, the CTB proteins were not specific for symbiotic and filamentous cyanobacteria, but some of the tandemly repeated genes radiated within the strains suggesting rapid adaptive evolution. The characteristic Nostoc transcript profiles confirmed that the ALC are akinetes.

3.8 | Profiles of polyA-enriched RNA from leaf-pocket preparations are consistent with expected metabolic activities in cells lining the leaf cavities

We next researched the physiological response of the fern to cornicinine by sequencing fern transcripts from isolated leaf cavities (leaf pockets). Leaf-pocket preparations were highly enriched in trichomes presumed to mediate fern-cyanobiont interactions (Figure 6a). We thus profiled RNA in ferns treated with(out) 500 nM cornicinine for 6 days, before the Nostoc akinetes were homogenously induced (Figure 6b,c). Despite polyA-enrichment a large proportion of read pairs sequenced from the leaf-pocket samples consisted of multi-mappers aligning to the Nostoc genome, mostly stemming from rRNA. As a result, the read pairs that mapped in a unique location to the fern genome varied from 1.3 to 7.5 million PE reads for the leaf-pocket samples (Figure 6d). Nevertheless, known functions of the 30 transcripts accumulating most highly and specifically in leaf-pocket preparations compared to sporophytes were consistent with activities expected from cells lining the leaf cavities (Figure 6e, sp vs. lp): reduced photosynthesis, increased secondary metabolism and transport.

Transcripts accumulating very highly in the leaf-pocket profiles of untreated ferns encoded enzymes critical for N-assimilation (Figure 7a,b): a cytosolic glutamine synthetase, specifically expressed in the leaf pockets, reaching the twelfth highest read counts in the leaf-pocket profile (Figure 7a, GS1 Afi_v2_s3215G000080.1), an asparagine synthetase (Figure 7a, ASN Afi_v2_s35G001910.1) and a NADH-dependent glutamate synthase (Figure 7a, GOGAT Afi_v2_s35G000930.1). In contrast, transcripts of nitrate reduction were little expressed, consistent with reports identifying ammonium as the likely metabolite secreted by Nostoc (Ray et al., 1978). The accumulation of the amino acid transporter LHT (Figure 7a, LHT Afi_v2_s23G003000.2) could reflect amino-acid export from the cells lining the leaf cavities. Moreover, leaf-pocket profiles had very high read counts for transcripts from key enzymes of flavonoid biosynthesis which is very active in trichomes lining the leaf cavity (Güngör et al., 2021; Pereira and Carrapiço, 2007; Tran et al., 2020). Leucoanthocyanidin reductase had the second highest read counts in the leaf-pocket profiles (Figure 7c, LAR Afi_v2_s74G000210.2), and two 2OGD resembling anthocyanidin synthase also had high transcript accumulation (Figure 7c, 2OGD Afi_v2_s16G002830.1 and Afi_v2_s44G002700.1). Having established a sense of trust in the noisy signal from the leaf-pocket profiles, we proceeded with comparing the leaf-pocket profiles obtained from ferns grown with (out) cornicinine.

3.9 | Fern leaf-cavity transcripts accumulating when akinetes are induced

Transcripts accumulating in leaf pockets from ferns with cornicinine versus without were few; the robust accumulation of transcripts encoding

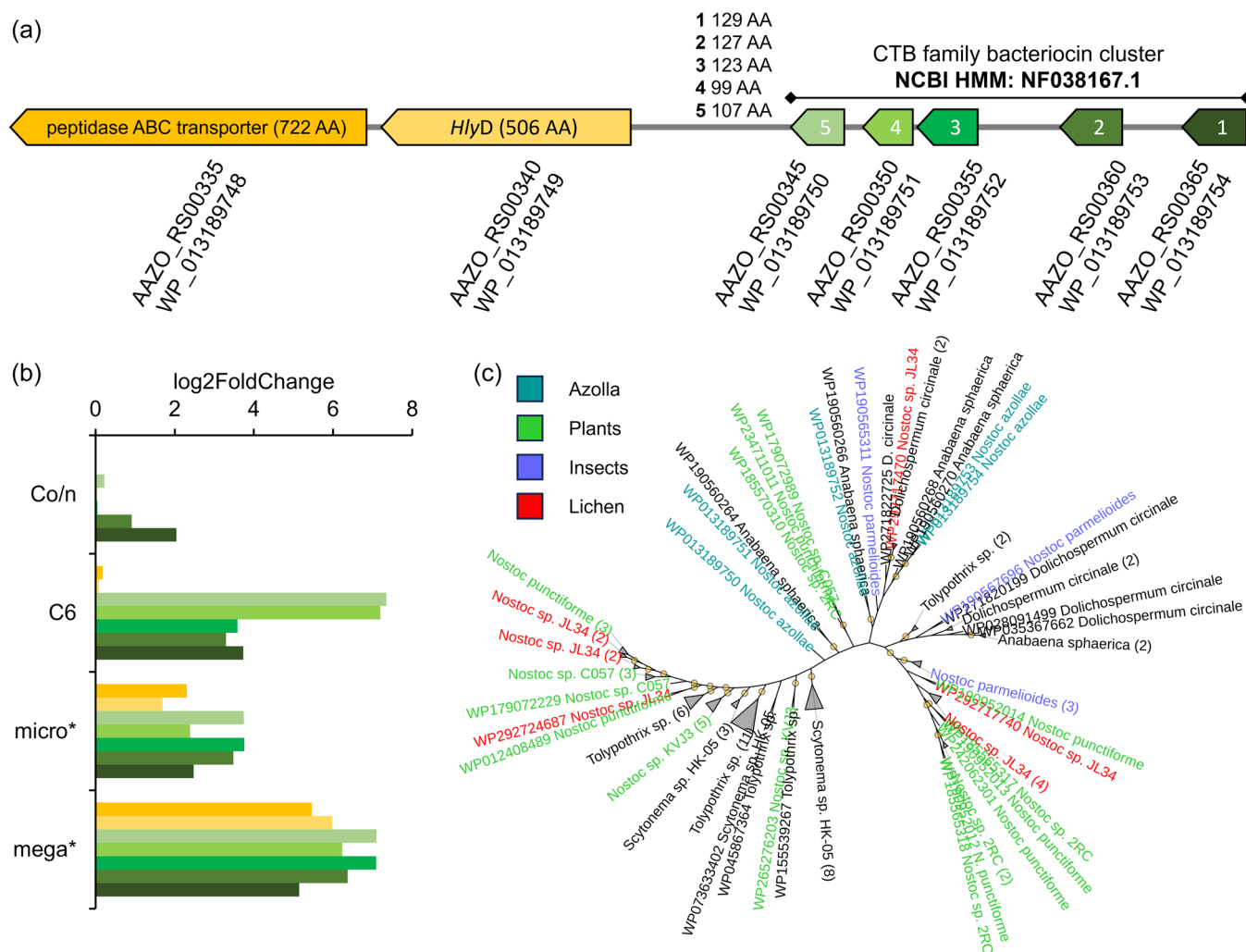


FIGURE 5 The CTB-family bacteriocin cluster differentially regulated in *Nostoc azollae* akinetes. (a) locus on the chromosome encoding the cluster. The CTB genes encode polypeptides with a leader sequence cleaved by the peptidase encoded by the ABC transporter. (b) Transcript accumulation of the CTB genes from (a) Log2FoldChange of reads assigned to *N. azollae* transcripts were from dual RNA-Seq comparing firstly, megasporocarps (mega*), microsporocarps (micro*) with sporophytes and secondly, sporophytes grown with and without cornicinine (500 nM; either overnight, Co/n, or six days, C6). (c) Phylogeny of CTB family bacteriocins (NCBI HMM accession NF038167.1) from free-living filamentous cyanobacteria and symbionts of plants, insects and lichen. Numbers in brackets refer to the number of genes in the collapsed clade of tandemly repeated genes from one strain; branches with a yellow circle have more than 90% bootstrap support. [Color figure can be viewed at [wileyonlinelibrary.com](https://onlinelibrary.wiley.com/doi/10.1111/pcel.14907)]

several components of the Cullin-RING ubiquitin ligase (CRUL) complexes in leaf pockets from ferns grown with cornicinine was, therefore, striking (Figure 7d). These components included F-box protein SKIP16-like (Afi_v2_s16G001530.1), and components of E2 and E3 ligases including the ATG12-like protein (Afi_v2_s49G00130.3) known to be involved in autophagy.

Host-genes associated with the formation of *bona fide* akinetes in megasporocarps were compared to those induced in sporophytes on cornicinine (File S2). This identified the sulfate transporter (Afi_v2_s23G003630.1), the 2OGD (Afi_v2_s44G002700.1) and tetra-spanin 8 (Afi_v2_s40G002850.2) as loci with high expression in fern tissues lining *Nostoc* akinetes (Figure 7e). Three DOXC-class 2OGDs (Afi_v2_s16G002830.1, Afi_v2_s44G002700.1; Afi_v2_s19G001900.6) were induced in the leaf cavities of ferns on cornicinine, but only

Afi_v2_s44G002700.1 (2OGD-s44) was also upregulated in the mega-sporocarp (Figure 8a).

Our phylogenomic analyses ascertained that the 2OGD-s44 enzyme unlikely catalyzes conversions of flavonoids (Figure S11). 2OGD-s44 belonged to a clade well-supported by bootstrapping (98% bootstrap) with representatives from ferns, gymnosperms and angiosperms (Figure 8b). The only functionally characterized angiosperm enzymes the clade contained were jasmonic acid oxidase (JOX) 1–4 from *Arabidopsis* (Figure 8b). The JOX were also the only *Arabidopsis* enzymes in the clade, suggesting that the clade represents enzymes accepting only jasmonic acid as substrate (with 2-oxoglutarate driving the redox reaction). Protein alignments revealed that the amino acids reported to interact with JA were conserved in the 2OGD-s44 which confirms it as a very likely JOX (Figure S12).

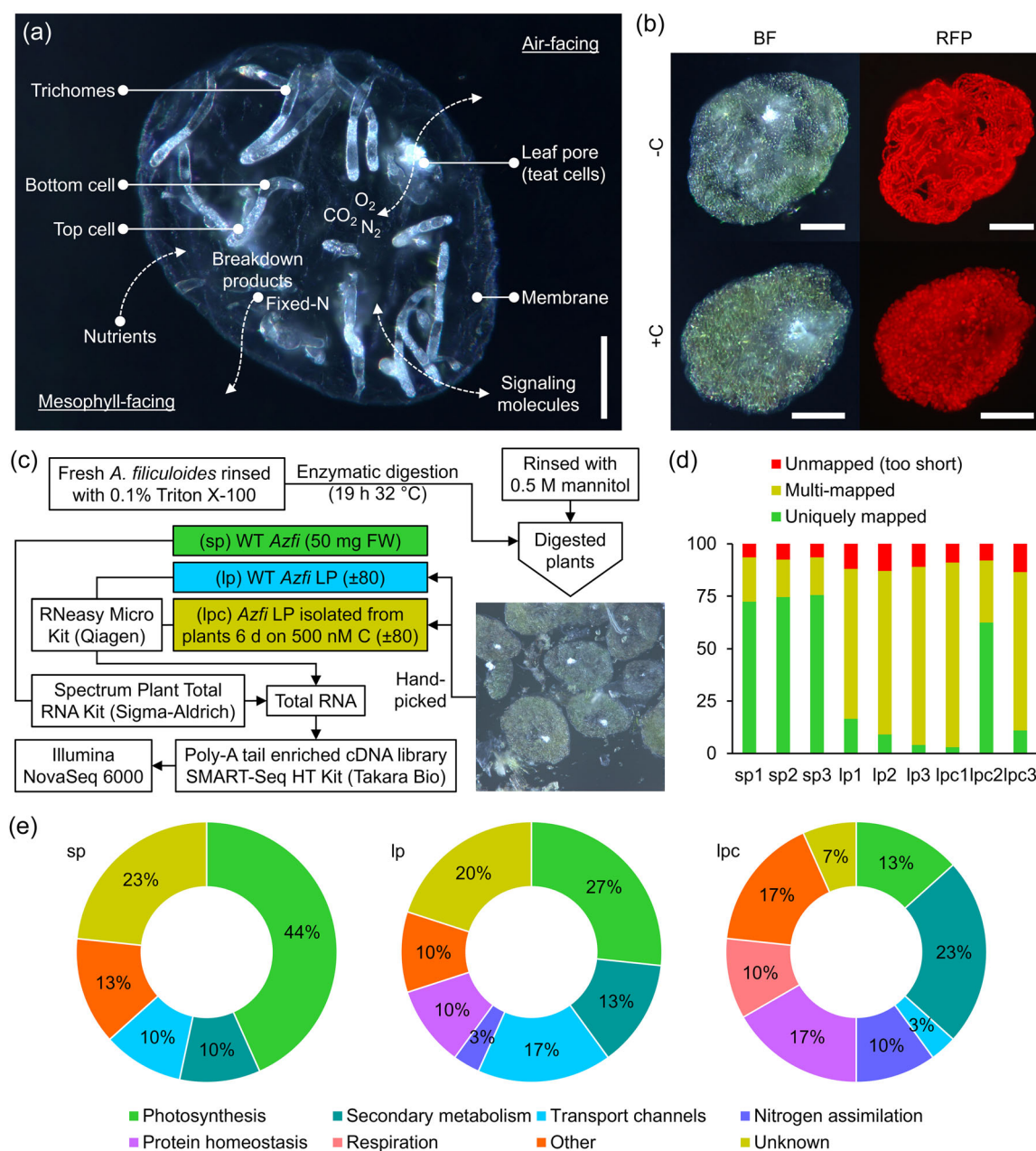


FIGURE 6 Transcription profiles of cells lining the leaf cavity in *A. filiculoides*. (a) Morphology of an empty leaf pocket prepared from *A. filiculoides* devoid Nostoc. The leaf pore with characteristic teat cells is air-facing while the trichomes emerge from the mesophyll-facing side. Scale bar corresponds to 100 μ m. (b) Leaf pockets prepared from sporophytes grown without (-C) and with 500 nM cornicinine (+C) for 10 days. BF: brightfield; RFP: fluorescence under RFP settings. Scale bars correspond to 50 μ m. (c) mRNA profiling of sporophyte (sp), leaf pockets (lp) and leaf pockets isolated from cornicinine-treated ferns (lpc). Sporophytes were treated 6 days with(out) 500 nM cornicinine; the leaf cavities were released enzymatically, then manually collected in three independent replicates per condition. All samples were collected snap frozen 2–3 h into the light period. Total RNA was extracted, DNase treated, enriched for poly-A tail before library preparation and sequencing. (d) Proportion of paired-end reads aligning to the concatenated genomes of *A. filiculoides*, its chloroplast, and *Nostoc azollae* using default settings of STAR aligner. (e) Functional categories of the 30 genes with highest transcript accumulation per sample type. [Color figure can be viewed at [wileyonlinelibrary.com](https://onlinelibrary.wiley.com/doi/10.1111/pcp.14907)]

4 | DISCUSSION

4.1 | The glycosylated trans-A triketide δ -lactone from insects is a semiochemical novelty

Insects are known to recruit metabolic capabilities from bacteria and therefore are a rich source of allelopathic chemicals, compounds that

mediate environmental signaling (Davis et al., 2013; Ferrari and Vavre, 2011). We have yet to reveal the ecological function of cornicinine and therefore cannot call it allelopathic. Its specific occurrence in the *N. cornicina* species and its specific activity on *Azolla* ferns sharing the wetland habitat suggest that cornicinine is a semiochemical. It is not volatile, however, and accumulates in the crane flies at levels much higher than would be expected from a pheromone. Its systematic association

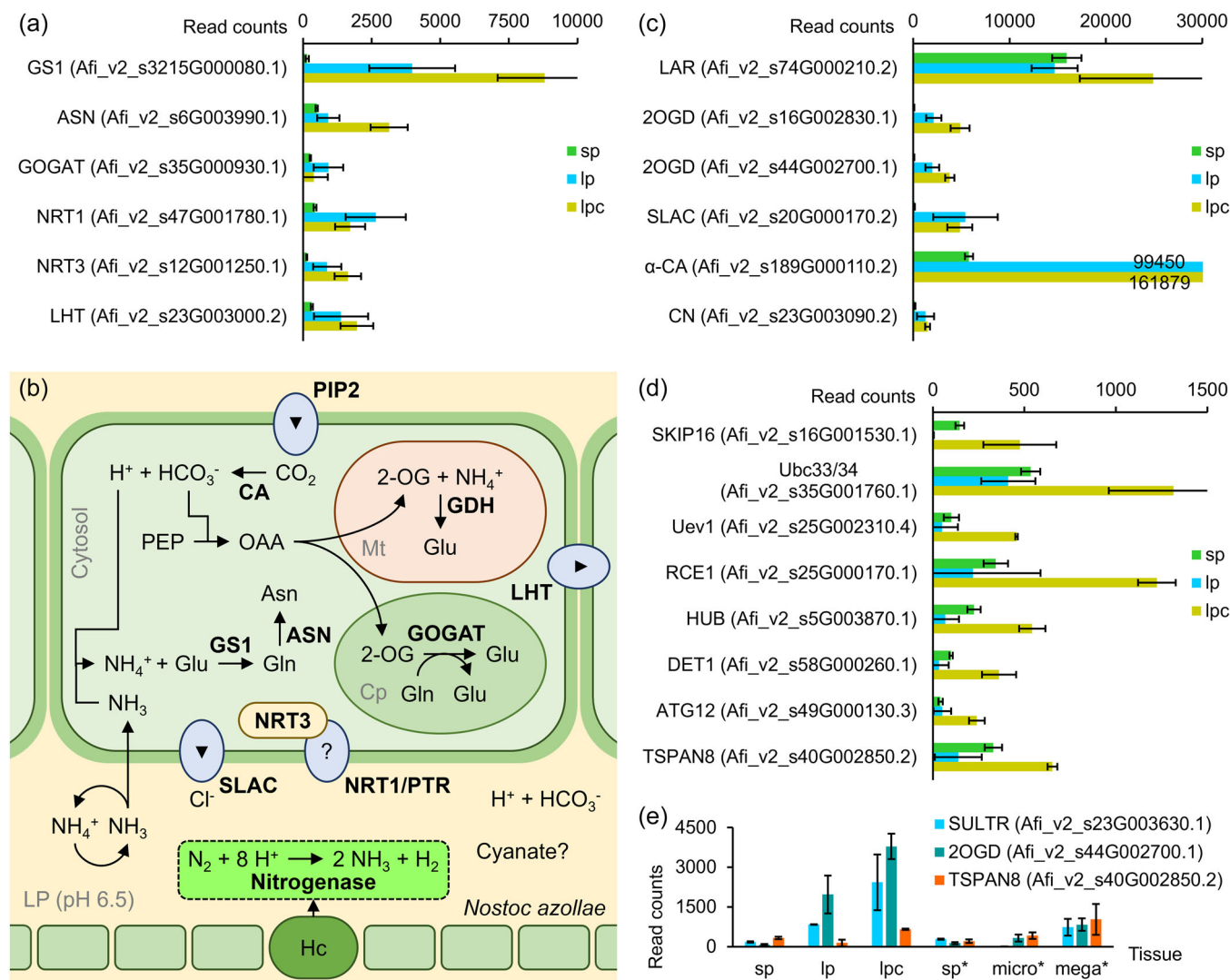


FIGURE 7 Abundant leaf-cavity transcripts related to nitrogen uptake, secondary metabolism, and responsive to cornicinine. (a) Ammonium assimilation and transport of nitrogenous products. (b) Proposed pathway for $\text{NH}_4^+/\text{NH}_3$ assimilation in fern cells lining the leaf cavity. (c) Secondary metabolism and CO_2 solvation. (d) Cornicinine responsive transcripts encoding F-box and ubiquitin ligase components or vesicle trafficking. α -CA, α -carbonic anhydrase; GS1, glutamine synthetase; ASN, aspartate aminotransferase; GDH, glutamate dioxygenase; GOGAT, glutamine oxoglutarate aminotransferase; SLAC, slow anion channel; LHT, neutral amino acid or ACC transporter; PIP2, plasma membrane intrinsic protein; NRT1/PTR transporters for NO_3^- , peptide or other solute. (e) Leaf-cavity specific transcripts responsive to cornicinine and upregulated in megasporocarps. *The samples were from a separate experiment profiling sporophytes (sp*), microsporocarps (micro*) and megasporocarps (mega*). Samples were collected as triplicate biological replicates 2 h into the 16 h light period. Standard deviations are shown for $n = 3$, except for lpc where $n = 2$. [Color figure can be viewed at [wileyonlinelibrary.com](https://onlinelibrary.wiley.com/doi/10.1111/pcpe.14907)]

with adult *N. cornicina* collected through the insect's wide range of distribution (Figure S1C) suggests that the crane fly synthesizes cornicinine with its own PKS. Recently, PKS were implicated in the biosynthesis of carminic acid, the red colorant from the cuticle of cochineal insects including *Dactylopius coccus* (Frandsen et al., 2018; Yang et al., 2021). PKS from animals including insects, however, have yet to be characterized (Frandsen et al., 2018).

Polyketide semiochemicals for which the biosynthesis pathway has been characterized thus far, have been synthesized by bacteria or fungi associated with insects. In some cases the microbes were insect defensive symbionts (Oliver and Perlman, 2020; van Moll et al., 2021).

However, polyketides synthesized by microbes associated with insects were generally more complex than the comparatively small cornicinine aglycone with m/z 170. An example is the polyketide lagriamide of m/z 750 synthesized by the *Burkholderia* species associated with the beetle *Lagriella villosa* (Flórez et al., 2018).

Cornicinine, a reduced triketide with a single glucose attached, resembles the simple polyketides synthesized by *Gerbera hybrida* plants, gerberin and parasorboside, identified as markers for the protection of the plants against Oomycetes (Mascellani et al., 2022). Cornicinine has previously been extracted from the flowers of *Centaurea parviflora* that belong to the family of the Asteraceae as

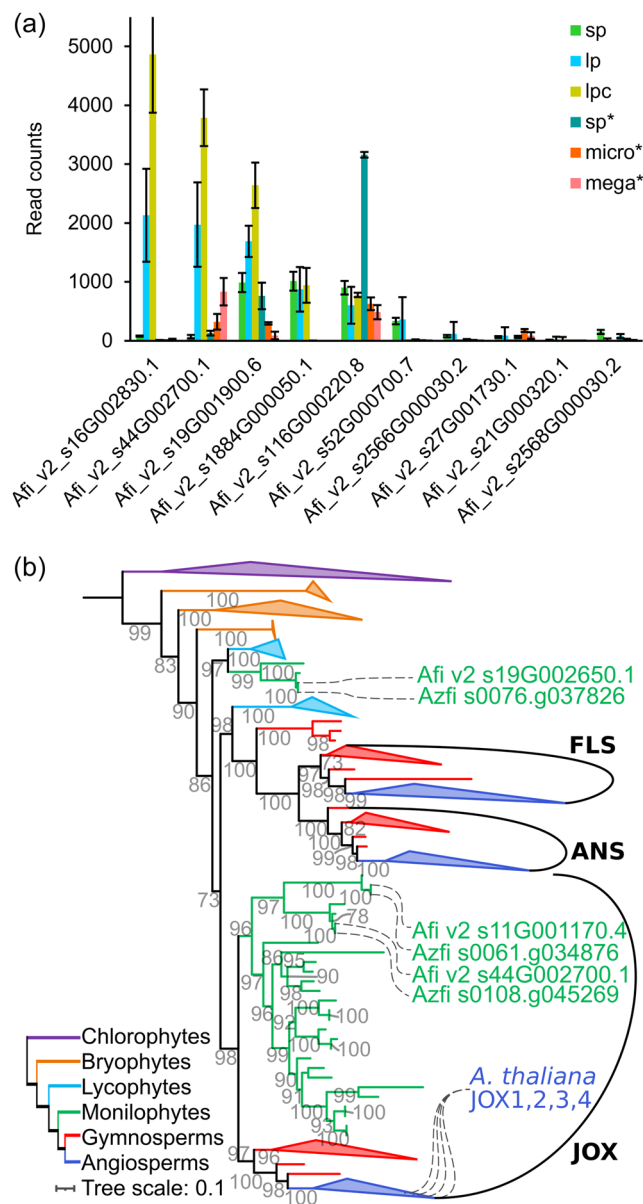


FIGURE 8 Expression and phylogeny of the DOXC enzymes from *Azolla*. (a) Ten most *Azolla* DOXC expressed in the leaf pockets. Samples were as in Figure 6e. (b) Phylogeny of 2OGD genes encoding FLS, ANS and JOX across land plant lineages. An initial phylogeny (Figure S11) was computed to place *A. filiculoides* genes in the broad 2OGD phylogeny. From this broad phylogeny, FLS, ANS, JOX and outgroup sequences were selected to compute a more accurate tree. Sequences were aligned with MAFFT-einsi (Katoh et al., 2019), and then trimmed using trimAL (Capella-Gutiérrez et al., 2009). The phylogeny was computed with IQ-tree (Nguyen et al., 2015) with 200 nonparametric bootstraps and transfer-bootstrap values were calculated with booster (Lemoine et al., 2018). JOX, jasmonic acid oxidase. [Color figure can be viewed at [wileyonlinelibrary.com](https://onlinelibrary.wiley.com/doi/10.1111/pcel.14907)]

does *G. hybrida* (Belkacem et al., 2014). The PKS for the biosynthesis of *G. hybrida* triketides has been identified as well as the accessory enzymes for reduction of the pyrone which actually occurs before cyclization (Zhu et al., 2022). Accumulation of cornicinine in the crane

fly and its larvae could thus also result from its feeding behavior. Identification of the PKS in the biosynthesis of cornicinine will reveal which organism synthesizes the compound in the future. The enzyme is of particular interest because a PKS synthesizing the R,R-triketide-lactone as in cornicinine has not been described: the PKS from antibiotic modules have proven very selective and difficult to engineer for a broader variety of substrates (Yin et al., 2003). PKS with novel properties have important applications to engineer novel polyketide drugs in pharmacology and (bio)pesticides in agriculture (Li et al., 2021). As such cornicinine could serve as the starting point for developing an *Azolla*-specific herbicide. Inactivity of the aglycone from cornicinine is consistent with previous results: polyketides require glycosylation for increased activity, uptake and transport, or stability (Mrudulakumari Vasudevan & Lee, 2020).

4.2 | Do fern trichomes lining the leaf cavities mediate the response to cornicinine?

High expression of the LAR in the leaf-pocket preparations is linked to the trichomes since proanthocyanins accumulate there and it may further be linked to the high JA-oxidase expression (Figure 7 and 8; Tran et al., 2020). In angiosperms, the link between JA elicitation and increased flavonoid accumulation is known and that between microbes inducing the JA-pathway and flavonoid accumulation is also well established (Albert et al., 2018; Chang et al., 2021). JA-control of glandular trichome differentiation and secondary metabolism is particularly well documented in tomato, but also found in artemisia (Ma et al., 2018; Xu et al., 2018). In contrast, bryophytes lack key enzymes of JA-Ile biosynthesis from the 12-oxo-phytodienoic acid precursor (OPDA). This includes *Marchantia polymorpha* that was reported to instead use OPDA-mediated signaling, thus not requiring JA-oxidase enzymes (Soriano et al., 2022). Consistently, the JA-oxidase clade supported with a bootstrap value of 98 (Figure 8b) did not contain sequences from the bryophytes and lycophytes; JA oxidation by JOX, therefore, evolved (likely by gene duplication and neofunctionalization) in the last common ancestor of ferns and angiosperms. A particularly interesting finding from the DOXC phylogeny (Figure 8b, Figure S11) was the position of the FLS/ANS-clade of enzymes from the flavonoid biosynthesis as a sister clade to the JOX clade suggesting that the JOX and FLS/ANS evolved from an ancestor enzyme, by gene duplication, in the common ancestor of ferns and lycophytes, which may explain commonalities in their regulation. To more definitely imply a role of the trichomes in mediating akinete differentiation, localization of the JOX (transcripts) inside trichomes is necessary.

4.3 | Cornicinine may function as an elicitor involving JA-metabolites

Many instances have been reported wherein semiochemicals from insects or plants alter bacteria physiology, yet in the present case the

signal likely is host mediated because it only altered the cyanobiont, not free-living cyanobacteria. Also, leaf-cavities with characteristic trichomes develop in *Azolla* in the absence of the cyanobiont (Figure 6a).

The mechanism of host-control over the differentiation of *Nostoc* may involve the plant JA-pathway because of the high and specific expression of a JA-oxidase in host cells lining the akinetes when ferns were exposed to cornicinine and in megasporocarps. Accumulation of RNA encoding a glycolipid transferase (Afi_v2_s3G001030.2) and an allene oxidase cyclase (Afi_v2_s28G002320.3) in the leaf cavities of ferns on cornicinine suggested increased JA-synthesis and turnover into 12-OH-JA or 12-OH-JA-Ile (File S2). Given that methyl jasmonate seemed ineffective in *Azolla*, the hydroxylated JA forms may be the active metabolite (de Vries et al., 2018): 12-OH-JA-Ile was recently shown to be an active JA form causing accumulation of anthocyanins in tomato and sorghum (Poudel et al., 2019). If the accumulation of active JA forms stretched to the whole leaf this would be consistent with cornicinine-induced leaf chlorosis (Jiang et al., 2014).

JA is a known player in plant immunity and its pathway may have been co-opted for symbiosis crosstalk in *Azolla*. Since the JA/SA pathway antagonism has been documented in bryophytes such as *Marchantia polymorpha*, we could expect both pathways to be active in the pteridophyte lineage and thus in the *Azolla* fern host. Indeed, *Marchantia* reacted to necrotrophic and biotrophic pathogens with either JA/SA pathway in a manner similar to what is predicted from seed plants (Matsui et al., 2020). The CRUL JA-receptor component COI1 is present in bryophytes, but JA-receptors have yet to be characterized using the most advanced *A. filiculoides* genome annotation (Afi_v2) released with this study. Receptors has been inferred by homology predictions in these ferns (de Vries et al., 2018).

Plants are known to perceive small molecules by way of CRUL complexes (Harper and Schulman, 2021). Even simple metabolites such as quinone were shown to be sensed by CRUL (Laohavisit et al., 2020). The ominous accumulation of transcripts encoding several components of such system in the leaf cavities of cornicinine grown ferns but not in megasporocarps (Figure 7d) suggests that cornicinine may be sensed by a CRUL complex and thus may function as an elicitor. Elicitors from insects that trigger plant immunity have been characterized mostly from grazing and sucking insect pests but not crane flies (Jones et al., 2022; Santamaria et al., 2018). They are not generally volatile, they identified as peptides, fatty acid derivatives, for example fatty acid conjugated to glutamine or glutamate (FACS), or hydroxypropanoate esters of long-chain α , ω -diols. FACS accumulate at substantial levels because of their role in nitrogen assimilation in the insect gut (Yoshinaga et al., 2008). Responses to insect elicitors are specific for each system and stage (herbivory, oviposition), but were often associated with altered JA-accumulation. Cornicinine elicitation reduces nitrogen fixation because it induces akinete formation (Figure 3); reduced plant nitrogen may have evolved to reduce the fitness of the crane-fly

larvae which would presumably feed on the *Azolla* canopy once hatched. Alternatively, considering the high accumulation of cornicinine in adult crane flies (0.1% DW), its production likely provides a positive selective advantage for the crane fly, which we have yet to identify. Given the shared habitat of the ferns and the crane fly, cornicinine may have evolved in the crane fly so as to co-opt the *Azolla*-symbiont signaling pathway and allow the adult crane fly to help ensure the fitness of its larval offspring. The larvae could benefit, for example, from reduced fitness of the plant or cyanobacteria within it, or from increased oxygen under the canopy of the growth arrested chlorotic ferns.

4.4 | If JA mediates cornicinine elicitation via JOX, what is the fern response to cornicinine causing akinetes to form?

Transcripts encoding the sulfate transporter and the tetraspanin 8 accumulated in fern tissues where akinetes form. Sulfate or the lack of it has previously been shown to induce akinete formation, for example, in *Nostoc* ANTH, a symbiotic strain known to colonize the roots of rice plants (Kyndiah and Rai, 2007; Wolk, 1965). Moreover, the sulfate transporter was listed in the repertoire of key genes specific for all symbiotic species of *Nostoc* (Warshan et al., 2018). Epiphytic colonization of ^{33}S -labelled moss gametophytes showed furthermore that S-compounds are transferred to the *Nostoc punctiforme* from the feathermoss *Pleurozium schreberi* (Stuart et al., 2020).

Electron microscopy revealed membrane vesicles (MV) surrounding *Nostoc* upon akinete formation in the megaspore indusium chamber from *A. microphylla* (Zheng et al., 2009). Images obtained after immunogold labeling demonstrate *Nostoc* cells fused with MV containing nucleic acids. Arabidopsis tetraspanin 8 knockout mutants were shown to secrete fewer extracellular vesicles than the wild types and such MV were found to contain small RNA that target fungal pathogens (Cai et al., 2018; Liu et al., 2020; Regente et al., 2017). The upregulation of tetraspanin 8 transcript in this study suggests that MV release is by the fern and facilitated by tetraspanin 8. Their content in nucleic acid is of particular interest because nucleic acids have been identified as a key in the maintenance of a phototrophic endosymbiosis: rRNA digestion products from the symbiont inhibit key transcriptional activity of the host which links symbiont rRNA turnover with host vigor (Jenkins et al., 2021).

CTB-bacteriocin secretion by the *Nostoc* akinetes may influence the host cells, antagonize competing bacteria in leaf cavities, meristem and indusium cap or maintain the akinete differentiation by way of an auto-inducing mechanism. The CTB-family belongs to class II bacteriocins of roughly 60 aa some of which form membrane pores in hosts and/or have auto-inducing activity. Experimental evidence for the activity of the CTB from cyanobacteria is lacking even though they were already identified and classified in 2011 (Wang et al., 2011).

4.5 | No trace of a fern host ammonium transporter but sky-rocketing read numbers encoding an α -carbonic anhydrase and a SLAC channel in cells lining the leaf cavity

In ferns without cornicine, transcripts of AMT transporters or NOD26, known to transport ammonium/ammonia did not accumulate in leaf pockets (Figure S13), in spite of predictions from other N_2 -fixing symbioses (Hwang et al., 2010). NH_4^+/NH_3 import may rely on the pH of the leaf cavity (Figure 7b). The pH surrounding symbiotic *Nostoc* was shown to be of importance in a symbiosis of peatmoss with *Nostoc muscorum* (Carrell et al., 2022). The pH of *Azolla* leaf cavities was reported to be 6.5 in leaves wherein *Nostoc* actively fixes N_2 . NH_3 converted from the NH_4 at this pH may not need a transport mechanism for uptake into the plant cell (Canini et al., 1992). Alternatively, an as yet uncharacterized transporter of cations imports NH_4^+ or an altogether differing mechanism may be involved given the strikingly high and leaf cavity specific accumulation of the NRT1/PTR (Afi_v2_s47G001780.1) transporter and NRT3 (Afi_v2_s12G001250.1) generally associated with nitrate transport and its regulation (Figure 7a). Nitrate may be synthesized via nitrogen oxide (NO) production from polyamines, hydroxylamine or arginine; the latter is synthesized in abundance. NO production and respiration was shown to be a pre-requisite for efficient N_2 -fixation in nodules from rhizobia (Valkov et al., 2020).

The extraordinary numbers of reads from the SLAC (Figure 7c, SLAC Afi_v2_s20G000170.2) and the α -carbonic anhydrase (Figure 7c, α -CA Afi_v2_s189G000110.2) are reminiscent of guard cell metabolism. Studies of the test cells that line leaf cavity pores suggest that they control gas exchange which would be crucial to maintain CO_2 and N_2 in the leaf cavity (Veys et al., 1999, 2000, 2002). The sky rocketing levels of an α -carbonic anhydrase and a SLAC transcript in the LP profiles may thus stem from the leaf cavity pore, the opening of which may be dynamically controlled as in the case of stomata.

ACKNOWLEDGEMENTS

We would like to thank Pjotr Oosterbroek for taxonomic assignments and for his help in contacting entomologists who provided *Nephrotoma cornicina* from various parts of the world. We thank Pasquale Ciliberti from Naturalis Biodiversity Center (Leiden, Netherlands) and Henk Bolhuis from Royal Netherlands Institute for Sea Research (Texel, Netherlands) for sharing *N. cornicina* crane fly specimens, and free-living filamentous cyanobacteria respectively. We further would like to thank Nils Stein for hosting the HiC work and Ines Walde for her technical help on the HiC library preparations and sequencing at the IPK (Seeland, Germany).

DATA AVAILABILITY STATEMENT

The data that support the findings of this study are openly available in ENA at <https://www.ebi.ac.uk>, reference number PRJEB60092.

ORCID

Erbil Güngör  <http://orcid.org/0000-0001-9612-2237>

Laura W. Dijkhuizen  <http://orcid.org/0000-0002-4628-7671>

Martin Mascher  <http://orcid.org/0000-0001-6373-6013>

Henriette Schluepmann  <http://orcid.org/0000-0001-6171-3029>

REFERENCES

- Albert, N.W., Thrimawithana, A.H., McGhie, T.K., Clayton, W.A., Deroles, S.C., Schwinn, K.E. et al. (2018) Genetic analysis of the liverwort *Marchantia polymorpha* reveals that R2R3MYB activation of flavonoid production in response to abiotic stress is an ancient character in land plants. *New Phytologist*, 218, 554–566. Available from: <https://doi.org/10.1111/nph.15002>
- Belkacem, S., Belbache, H., Boubekri, C., Mosset, P., Rached-Mosbah, O., Marchioni, E. et al. (2014) Chemical constituents from centaurea parviflora desf. *Res J Pharm Biol Chem Sci*, 5, 1275–1279.
- Brinkhuis, H., Schouten, S., Collinson, M.E., Sluijs, A., Damsté, J.S.S., Dickens, G.R. et al. (2006) Episodic fresh surface waters in the eocene Arctic Ocean. *Nature*, 441, 606–609. Available from: <https://doi.org/10.1038/nature04692>
- Brouwer, P., Bräutigam, A., Buijs, V.A., Tazelaar, A.O.E., van der Werf, A., Schlüter, U. et al. (2017) Metabolic adaptation, a specialized leaf organ structure and vascular responses to diurnal N_2 fixation by *Nostoc azollae* sustain the astonishing productivity of azolla ferns without nitrogen fertilizer. *Frontiers in Plant Science*, 8, 442. Available from: <https://doi.org/10.3389/fpls.2017.00442>
- Cai, Q., Qiao, L., Wang, M., He, B., Lin, F.-M., Palmquist, J. et al. (2018) Plants send small RNAs in extracellular vesicles to fungal pathogen to silence virulence genes. *Science*, 360, 1126–1129. Available from: <https://doi.org/10.1126/science.aar4142>
- Calvert, H.E., Pence, M.K. & Peters, G.A. (1985) Ultrastructural ontogeny of leaf cavity trichomes in *Azolla* implies a functional role in metabolite exchange. *Protoplasma*, 129, 10–27. Available from: <https://doi.org/10.1007/BF01282301>
- Canini, A., Grilli Caiola, M., Bertocchi, P., Lavagnini, M.G. & Mascini, M. (1992) Ion determinations within *Azolla* leaf cavities by microelectrodes. *Sensors and Actuators B: Chemical*, 7, 431–435. Available from: [https://doi.org/10.1016/0925-4005\(92\)80338-X](https://doi.org/10.1016/0925-4005(92)80338-X)
- Capella-Gutiérrez, S., Silla-Martínez, J.M. & Gabaldón, T. (2009) trimAl: a tool for automated alignment trimming in large-scale phylogenetic analyses. *Bioinformatics*, 25, 1972–1973. Available from: <https://doi.org/10.1093/bioinformatics/btp348>
- Carrell, A.A., Veličković, D., Lawrence, T.J., Bowen, B.P., Louie, K.B., Carper, D.L. et al. (2022) Novel metabolic interactions and environmental conditions mediate the boreal peatmoss-Cyanobacteria mutualism. *The ISME Journal*, 16, 1074–1085. Available from: <https://doi.org/10.1038/s41396-021-01136-0>
- Chang, L., Wu, S. & Tian, L. (2021) Methyl jasmonate elicits distinctive hydrolyzable tannin, flavonoid, and phyto-oxylipin responses in pomegranate (*Punica granatum* L.) leaves. *Planta*, 254, 89. Available from: <https://doi.org/10.1007/s00425-021-03735-9>
- Chin, C.-S., Alexander, D.H., Marks, P., Klammer, A.A., Drake, J., Heiner, C. et al. (2013) Nonhybrid, finished microbial genome assemblies from long-read SMRT sequencing data. *Nature Methods*, 10, 563–569. Available from: <https://doi.org/10.1038/nmeth.2474>
- Cohen, M.F., Sakihama, Y., Takagi, Y.C., Ichiba, T. & Yamasaki, H. (2002) Synergistic effect of deoxyanthocyanins from symbiotic fern *Azolla* spp. on *hrmA* gene induction in the cyanobacterium *Nostoc punctiforme*. *Molecular Plant-Microbe Interactions*, 15, 875–882. Available from: <https://doi.org/10.1094/MPMI.2002.15.9.875>
- Davis, T.S., Crippen, T.L., Hofstetter, R.W. & Tomberlin, J.K. (2013) Microbial volatile emissions as insect semiochemicals. *Journal of*

- Chemical Ecology*, 39, 840–859. Available from: <https://doi.org/10.1007/s10886-013-0306-z>
- Dijkhuizen, L.W., Brouwer, P., Bolhuis, H., Reichart, G.-J., Koppers, N., Huettel, B. et al. (2018) Is there foul play in the leaf pocket? The metagenome of floating fern *Azolla* reveals endophytes that do not fix N₂ but May denitrify. *New Phytologist*, 217, 453–466. Available from: <https://doi.org/10.1111/nph.14843>
- Dijkhuizen, L.W., Tabatabaei, B.E.S., Brouwer, P., Rijken, N., Buijs, V.A., Güngör, E. et al. (2021) Far-Red Light-Induced *Azolla filiculoides* symbiosis sexual reproduction: responsive transcripts of symbiont *Nostoc azollae* encode transporters whilst those of the fern relate to the angiosperm floral transition. *Frontiers in Plant Science*, 12, 693039. Available from: <https://doi.org/10.3389/fpls.2021.693039>
- Dobin, A., Davis, C.A., Schlesinger, F., Drenkow, J., Zaleski, C., Jha, S. et al. (2013) STAR: ultrafast universal RNA-seq aligner. *Bioinformatics*, 29, 15–21. Available from: <https://doi.org/10.1093/bioinformatics/bts635>
- Dunham, D.G. & Fowler, K. (1987) Megaspore germination, embryo development and maintenance of the symbiotic association in *Azolla filiculoides* Lam. *Botanical Journal of the Linnean Society*, 95, 43–53. Available from: <https://doi.org/10.1111/j.1095-8339.1987.tb01835.x>
- Feldhaar, H. (2011) Bacterial symbionts as mediators of ecologically important traits of insect hosts. *Ecological Entomology*, 36, 533–543. Available from: <https://doi.org/10.1111/j.1365-2311.2011.01318.x>
- Ferrari, J. & Vavre, F. (2011) Bacterial symbionts in insects or the story of communities affecting communities. *Philosophical Transactions of the Royal Society, B: Biological Sciences*, 366, 1389–1400. Available from: <https://doi.org/10.1098/rstb.2010.0226>
- Flórez, L.v., Scherlach, K., Miller, I.J., Rodrigues, A., Kwan, J.C. & Hertweck, C. et al. (2018) An antifungal polyketide associated with horizontally acquired genes supports symbiont-mediated defense in *Lagria villosa* beetles. *Nature Communications*, 9, 2478. <https://doi.org/10.1038/s41467-018-04955-6>
- Frandsen, R.J.N., Khorsand-Jamal, P., Kongstad, K.T., Nafisi, M., Kannangara, R.M., Staerk, D. et al. (2018) Heterologous production of the widely used natural food colorant carminic acid in *Aspergillus nidulans*. *Scientific Reports*, 8, 12853. Available from: <https://doi.org/10.1038/s41598-018-30816-9>
- Güngör, E., Brouwer, P., Dijkhuizen, L.W., Shaffar, D.C., Nierop, K.G.J., de Vos, R.C.H. et al. (2021) *Azolla* ferns testify: seed plants and ferns share a common ancestor for leucoanthocyanidin reductase enzymes. *New Phytologist*, 229, 1118–1132. Available from: <https://doi.org/10.1111/nph.16896>
- Harper, J.W. & Schulman, B.A. (2021) Cullin-RING ubiquitin ligase regulatory circuits: a quarter century beyond the F-Box hypothesis. *Annual Review of Biochemistry*, 90, 403–429. Available from: <https://doi.org/10.1146/annurev-biochem-090120-013613>
- Hashidoko, Y., Nishizuka, H., Tanaka, M., Murata, K., Murai, Y. & Hashimoto, M. (2019) Isolation and characterization of 1-palmitoyl-2-linoleoyl-sn-glycerol as a hormogonium-inducing factor (HIF) from the coralloid roots of *Cycas revoluta* (Cycadaceae). *Scientific Reports*, 9, 4751. Available from: <https://doi.org/10.1038/s41598-019-39647-8>
- Himmelbach, A., Walde, I., Mascher, M. & Stein, N. (2018) Tethered chromosome conformation capture sequencing in *Triticeae*: A valuable tool for genome assembly. *BIO-PROTOCOL*, 8(15), e2955. Available from: <https://doi.org/10.21769/BioProtoc.2955>
- Hinterding, K., Singhanat, S. & Oberer, L. (2001) Stereoselective synthesis of polyketide fragments using a novel intramolecular Claisen-like condensation/reduction sequence. *Tetrahedron Letters*, 42, 8463–8465. Available from: [https://doi.org/10.1016/S0040-4039\(01\)01840-8](https://doi.org/10.1016/S0040-4039(01)01840-8)
- Hwang, J.H., Ellingson, S.R. & Roberts, D.M. (2010) Ammonia permeability of the soybean nodulin 26 channel. *FEBS Letters*, 584, 4339–4343. Available from: <https://doi.org/10.1016/j.febslet.2010.09.033>
- Jenkins, B.H., Maguire, F., Leonard, G., Eaton, J.D., West, S., Housden, B.E. et al. (2021) Emergent RNA–RNA interactions can promote stability in a facultative phototrophic endosymbiosis. *Proceedings of the National Academy of Sciences*, 118(38), e2108874118. Available from: <https://doi.org/10.1073/pnas.2108874118>
- Jiang, Y., Liang, G., Yang, S. & Yu, D. (2014) Arabidopsis WRKY57 functions as a node of convergence for jasmonic acid- and auxin-mediated signaling in jasmonic acid-induced leaf senescence. *The Plant Cell*, 26, 230–245. Available from: <https://doi.org/10.1105/tpc.113.117838>
- Jones, A.C., Felton, G.W. & Tumlinson, J.H. (2022) The dual function of elicitors and effectors from insects: reviewing the ‘arms race’ against plant defenses. *Plant Molecular Biology*, 109, 427–445. Available from: <https://doi.org/10.1007/s11103-021-01203-2>
- de Jong, H., Oosterbroek, P. & Beuk, P.L.T.h (2021) Family Tipulidae. Checklist of the Diptera of the Netherlands. Available from: http://www.diptera-info.nl/infusions/checklist/view_family.php?fam_id=9
- Ka-Shu Wong, G., Soltis, D.E., Leebens-Mack, J., Wickett, N.J., Barker, M.S. & van de Peer, Y. et al. (2019) Sequencing and Analyzing the Transcriptomes of a Thousand Species Across the Tree of Life for Green Plants. Available from: <https://doi.org/10.1146/annurev-arplant-042916>
- Katoh, K., Rozewicki, J. & Yamada, K.D. (2019) MAFFT online service: multiple sequence alignment, interactive sequence choice and visualization. *Briefings in Bioinformatics*, 20, 1160–1166. Available from: <https://doi.org/10.1093/bib/bbx108>
- Kawai, Y., Ono, E. & Mizutani, M. (2014) Evolution and diversity of the 2-oxoglutarate-dependent dioxygenase superfamily in plants. *The Plant Journal*, 78, 328–343. Available from: <https://doi.org/10.1111/tpj.12479>
- Keilwagen, J., Hartung, F. & Grau, J. (2019) GeMoMa: Homology-Based Gene Prediction Utilizing Intron Position Conservation and RNA-seq Data. 161–177. Available from: https://doi.org/10.1007/978-1-4939-9173-0_9
- Koren, S., Walenz, B.P., Berlin, K., Miller, J.R., Bergman, N.H. & Phillippy, A.M. (2017) Canu: scalable and accurate long-read assembly via adaptive k-mer weighting and repeat separation. *Genome Research*, 27, 722–736. Available from: <https://doi.org/10.1101/gr.215087.116>
- Kyndiah, O. & Rai, A.N. 2007. Induction of sporulation by sulphate limitation in *Nostoc ANTH*, a symbiotic strain capable of colonizing roots of rice plants.
- Laohavisit, A., Wakatake, T., Ishihama, N., Mulvey, H., Takizawa, K., Suzuki, T. et al. (2020) Quinone perception in plants via leucine-rich-repeat receptor-like kinases. *Nature*, 587, 92–97. Available from: <https://doi.org/10.1038/s41586-020-2655-4>
- Lemoine, F., Domelevo Entfellner, J.-B., Wilkinson, E., Correia, D., Dávila Felipe, M., de Oliveira, T. et al. (2018) Renewing Felsenstein's phylogenetic bootstrap in the era of big data. *Nature*, 556, 452–456. Available from: <https://doi.org/10.1038/s41586-018-0043-0>
- Letunic, I. & Bork, P. (2019) Interactive tree of life (iTOL) v4: recent updates and new developments. *Nucleic Acids Research*, 47, W256–W259. Available from: <https://doi.org/10.1093/nar/gkz239>
- Li, D.-D., Ni, R., Wang, P.-P., Zhang, X.-S., Wang, P.-Y., Zhu, T.-T. et al. (2020) Molecular basis for chemical evolution of flavones to flavonols and anthocyanins in land plants. *Plant Physiology*, 184, 1731–1743. Available from: <https://doi.org/10.1104/pp.20.01185>
- Li, F.-W., Brouwer, P., Carretero-Paulet, L., Cheng, S., de Vries, J., Delaux, P.-M. et al. (2018) Fern genomes elucidate land plant evolution and cyanobacterial symbioses. *Nature Plants*, 4, 460–472. Available from: <https://doi.org/10.1038/s41477-018-0188-8>

- Li, S., Yang, B., Tan, G.-Y., Ouyang, L.-M., Qiu, S., Wang, W. et al. (2021) Polyketide pesticides from actinomycetes. *Current Opinion in Biotechnology*, 69, 299–307. Available from: <https://doi.org/10.1016/j.copbio.2021.05.006>
- Liaimer, A., Helfrich, E.J.N., Hinrichs, K., Guljamow, A., Ishida, K., Hertweck, C. et al. (2015) Nostopeptolide plays a governing role during cellular differentiation of the symbiotic cyanobacterium *Nostoc punctiforme*. *Proceedings of the National Academy of Sciences*, 112, 1862–1867. Available from: <https://doi.org/10.1073/pnas.1419543112>
- Linnaeus, C. (1758). *Systema naturae* (Vol. 1, Part 1, p. 532). Laurentii Salvii: Stockholm.
- Liu, N.-J., Wang, N., Bao, J.-J., Zhu, H.-X., Wang, L.-J. & Chen, X.-Y. (2020) Lipidomic analysis reveals the importance of GIPCs in arabidopsis leaf extracellular vesicles. *Molecular Plant*, 13, 1523–1532. Available from: <https://doi.org/10.1016/j.molp.2020.07.016>
- Lohse, M., Nagel, A., Herter, T., May, P., Schroda, M., Zrenner, R. et al. (2014) Mercator: A fast and simple web server for genome scale functional annotation of plant sequence data. *Plant, Cell & Environment*, 37, 1250–1258. Available from: <https://doi.org/10.1111/pce.12231>
- Love, M.I., Huber, W. & Anders, S. (2014) Moderated estimation of fold change and dispersion for RNA-seq data with DESeq. 2. *Genome Biology*, 15(12), 550. Available from: <https://doi.org/10.1186/s13059-014-0550-8>
- Ma, Y.-N., Xu, D.-B., Li, L., Zhang, F., Fu, X.-Q., Shen, Q. et al. (2018) Jasmonate promotes artemisinin biosynthesis by activating the TCP14-ORA complex in *Artemisia annua*. *Science Advances*, 4, eaas9357. Available from: <https://doi.org/10.1126/sciadv.aas9357>
- Manni, M., Berkeley, M.R., Seppey, M., Simão, F.A. & Zdobnov, E.M. (2021) BUSCO update: novel and streamlined workflows along with broader and deeper phylogenetic coverage for scoring of eukaryotic, prokaryotic, and viral genomes. *Molecular Biology and Evolution*, 38, 4647–4654. Available from: <https://doi.org/10.1093/molbev/msab199>
- Mascellani, A., Leiss, K., Bac-Molenaar, J., Malanik, M., Marsik, P., Hernandez Olesinski, E. et al. (2022) Polyketide derivatives in the resistance of *Gerbera hybrida* to powdery mildew. *Frontiers in Plant Science*, 12, 790907. Available from: <https://doi.org/10.3389/fpls.2021.790907>
- Mascher, M., Gundlach, H., Himmelbach, A., Beier, S., Twardziok, S.O., Wicker, T. et al. (2017) A chromosome conformation capture ordered sequence of the barley genome. *Nature*, 544, 427–433. Available from: <https://doi.org/10.1038/nature22043>
- Mathieu, B., de Hoffmann, E. & van Hove, C. (2005) Glycosylated triketide delta lactones. *International Application Published Under the Patent Cooperation Treaty (PCT)*, Number WO, 54267, A1.
- Matsui, H., Iwakawa, H., Hyon, G.-S., Yotsui, I., Katou, S., Monte, I. et al. (2020) Isolation of natural fungal pathogens from *Marchantia polymorpha* reveals antagonism between salicylic acid and jasmonate during Liverwort–Fungus interactions. *Plant and Cell Physiology*, 61, 265–275. Available from: <https://doi.org/10.1093/pcp/pcz187>
- van Moll, L., de Smet, J., Cos, P. & van Campenhout, L. (2021) Microbial symbionts of insects as a source of new antimicrobials: a review. *Critical Reviews in Microbiology*, 47, 562–579. Available from: <https://doi.org/10.1080/1040841X.2021.1907302>
- Mrudulakumari Vasudevan, U. & Lee, E.Y. (2020) Flavonoids, terpenoids, and polyketide antibiotics: role of glycosylation and biocatalytic tactics in engineering glycosylation. *Biotechnology Advances*, 41, 107550. Available from: <https://doi.org/10.1016/j.biotechadv.2020.107550>
- Nguyen, L.-T., Schmidt, H.A., von Haeseler, A. & Minh, B.Q. (2015) IQ-TREE: A fast and effective stochastic algorithm for estimating maximum-likelihood phylogenies. *Molecular Biology and Evolution*, 32, 268–274. Available from: <https://doi.org/10.1093/molbev/msu300>
- Oliver, K.M. & Perlman, S.J. 2020. Toxin-mediated protection against natural enemies by insect defensive symbionts. 277–316. Available from: <https://doi.org/10.1016/bs.aip.2020.03.005>
- Pereira, A.L. & Carrapiço, F. (2007) Histochemistry of simple hairs from the foliar cavities of *Azolla filiculoides*. *Plant Biosystems—An International Journal Dealing with all Aspects of Plant Biology*, 141, 323–328. Available from: <https://doi.org/10.1080/11263500701627588>
- Perkins, S.K. & Peters, G.A. (2006) The *Azolla*-*Anabaena* symbiosis: endophyte continuity in the *Azolla* life-cycle is facilitated by epidermal trichomes. *New Phytologist*, 123, 53–64. Available from: <https://doi.org/10.1111/j.1469-8137.1993.tb04531.x>
- Peters, G.A. & Perkins, S.K. (2006) The *Azolla*-*Anabaena* symbiosis: endophyte continuity in the *Azolla* life-cycle is facilitated by epidermal trichomes. *New Phytologist*, 123, 65–75. Available from: <https://doi.org/10.1111/j.1469-8137.1993.tb04532.x>
- Peters, G.A., Toia, R.E., Raveed, D. & Levine, N.J. (1978) The *Azolla*-*Anabaena azollae* relationship. vi. morphological aspects of the association. *New Phytologist*, 80, 583–593. Available from: <https://doi.org/10.1111/j.1469-8137.1978.tb01591.x>
- Poudel, A.N., Holtsclaw, R.E., Kimberlin, A., Sen, S., Zeng, S., Joshi, T. et al. (2019) 12-Hydroxy-Jasmonoyl-L-Isoleucine is an active jasmonate that signals through CORONATINE INSENSITIVE 1 and contributes to the wound response in arabidopsis. *Plant and Cell Physiology*, 60, 2152–2166. Available from: <https://doi.org/10.1093/pcp/pcz109>
- Ray, T.B., Peters, G.A., Toia Jr., R.E. & Mayne, B.C. (1978) *Azolla*-*Anabaena* Relationships: VII. distribution of ammonia-assimilating enzymes, protein, and chlorophyll between host and symbiont. *Plant Physiology*, 62, 463–467. Available from: <https://doi.org/10.1104/pp.62.3.463>
- Regente, M., Pinedo, M., San Clemente, H., Balliau, T., Jamet, E. & de la Canal, L. (2017) Plant extracellular vesicles are incorporated by a fungal pathogen and inhibit its growth. *Journal of Experimental Botany*, 68, 5485–5495. Available from: <https://doi.org/10.1093/jxb/erx355>
- Santamaría, M., Arnaiz, A., Gonzalez-Melendi, P., Martinez, M. & Diaz, I. (2018) Plant perception and Short-Term responses to phytophagous insects and mites. *International Journal of Molecular Sciences*, 19, 1356. Available from: <https://doi.org/10.3390/ijms19051356>
- Schluepmann, H., Bigot, I., Rijken, N., Grifoll, A.C., Gudde, P.A., Dijkhuizen, L.W. et al. (2022) Domestication of the floating fern symbiosis *Azolla*. In *Ferns: Biotechnology, Propagation, Medicinal Uses and Environmental Regulation 2022 May 6*. Singapore: Springer Nature Singapore. pp. 149–180.
- Soriano, G., Kneeshaw, S., Jimenez-Aleman, G., Zamarreño, Á.M., Franco-Zorrilla, J.M., Rey-Stolle, F. et al. (2022) An evolutionarily ancient fatty acid desaturase is required for the synthesis of hexadecatrienoic acid, which is the main source of the bioactive jasmonate in *Marchantia polymorpha*. *New Phytologist*, 233, 1401–1413. Available from: <https://doi.org/10.1111/nph.17850>
- Stuart, R.K., Pederson, E.R.A., Weyman, P.D., Weber, P.K., Rassmussen, U. & Dupont, C.L. (2020) Bidirectional C and N transfer and a potential role for sulfur in an epiphytic diazotrophic mutualism. *The ISME journal*, 14, 3068–3078. Available from: <https://doi.org/10.1038/s41396-020-00738-4>
- Tran, T.L.N., Miranda, A.F., Abeynayake, S.W. & Mouradov, A. (2020) Differential production of phenolics, lipids, carbohydrates and proteins in stressed and unstressed aquatic plants, *Azolla filiculoides* and *Azolla pinnata*. *Biology*, 9, 342. Available from: <https://doi.org/10.3390/biology9100342>
- Uheda, E. (1986) Isolation of empty packets from *Anabaena*-free *Azolla*. *Plant and Cell Physiology*, 27, 1187–1190. Available from: <https://doi.org/10.1093/oxfordjournals.pcp.a077203>
- Valkov, V.T., Sol, S., Rogato, A. & Chiurazzi, M. (2020) The functional characterization of *LjNRT2.4* indicates a novel, positive role of nitrate

- for an efficient nodule N_2 -fixation activity. *New Phytologist*, 228, 682–696. Available from: <https://doi.org/10.1111/nph.16728>
- Veys, P., Lejeune, A. & van Hove, C. (2000) The pore of the leaf cavity of *Azolla*: interspecific morphological differences and continuity between the cavity envelopes. *Symbiosis*, 29, 33–47.
- Veys, P., Lejeune, A. & Hove, C.V. (2002) The pore of the leaf cavity of *Azolla* species: test cell differentiation and cell wall projections. *Protoplasma*, 219, 0031–0042. Available from: <https://doi.org/10.1007/s007090200003>
- Veys, P., Waterkeyn, L., Lejeune, A. & van Hove, C. (1999) The pore of the leaf cavity of *Azolla*: morphology, cytochemistry and possible functions. *Symbiosis*, 27, 33–57.
- de Vries, J., Fischer, A.M., Roettger, M., Rommel, S., Schlupepman, H., Bräutigam, A. et al. (2016) Cytokinin-induced promotion of root meristem size in the fern *Azolla* supports a shoot-like origin of euphyllophyte roots. *New Phytologist*, 209, 705–720. Available from: <https://doi.org/10.1111/nph.13630>
- de Vries, S., de Vries, J., Teschke, H., von Dahlen, J.K., Rose, L.E. & Gould, S.B. (2018) Jasmonic and salicylic acid response in the fern *Azolla filiculoides* and its cyanobiont. *Plant, Cell & Environment*, 41, 2530–2548. Available from: <https://doi.org/10.1111/pce.13131>
- Walker, B.J., Abeel, T., Shea, T., Priest, M., Abouelliel, A., Sakthikumar, S. et al. (2014) Pilon: an integrated tool for comprehensive microbial variant detection and genome assembly improvement. *PLoS One*, 9, e112963. Available from: <https://doi.org/10.1371/journal.pone.0112963>
- Wang, H., Fewer, D.P. & Sivonen, K. (2011) Genome mining demonstrates the widespread occurrence of gene clusters encoding bacteriocins in Cyanobacteria. *PLoS One*, 6(7), e22384. Available from: <https://doi.org/10.1371/journal.pone.0022384>
- Warshan, D., Liaimer, A., Pederson, E., Kim, S.-Y., Shapiro, N., Woyke, T. et al. (2018) Genomic changes associated with the evolutionary transitions of *Nostoc* to a plant symbiont. *Molecular Biology and Evolution*, 35, 1160–1175. Available from: <https://doi.org/10.1093/molbev/msy029>
- Wolk, C.P. (1965) Control of sporulation in a blue-Green alga. *Developmental Biology*, 12, 15–35. Available from: [https://doi.org/10.1016/0012-1606\(65\)90018-7](https://doi.org/10.1016/0012-1606(65)90018-7)
- Xu, J., van Herwijnen, Z.O., Dräger, D.B., Sui, C., Haring, M.A. & Schuurink, R.C. (2018) SIMYC1 regulates type VI glandular trichome formation and terpene biosynthesis in tomato glandular cells. *The Plant Cell*, 30, 2988–3005. Available from: <https://doi.org/10.1105/tpc.18.00571>
- Yang, D., Jang, W.D. & Lee, S.Y. (2021) Production of carminic acid by metabolically engineered *Escherichia coli*. *Journal of the American Chemical Society*, 143, 5364–5377. Available from: <https://doi.org/10.1021/jacs.0c12406>
- Yin, Y., Lu, H., Khosla, C. & Cane, D.E. (2003) Expression and kinetic analysis of the substrate specificity of modules 5 and 6 of the Picromycin/Methymycin polyketide synthase. *Journal of the American Chemical Society*, 125, 5671–5676. Available from: <https://doi.org/10.1021/ja034574q>
- Yoshinaga, N., Aboshi, T., Abe, H., Nishida, R., Alborn, H.T., Tumlinson, J.H. et al. (2008) Active role of fatty acid amino acid conjugates in nitrogen metabolism in *Spodoptera litura* larvae. *Proceedings of the National Academy of Sciences*, 105, 18058–18063. Available from: <https://doi.org/10.1073/pnas.0809623105>
- Zheng, W., Bergman, B., Chen, B., Zheng, S., Xiang, G. & Rasmussen, U. (2009) Cellular responses in the cyanobacterial symbiont during its vertical transfer between plant generations in the *Azolla microphylla* symbiosis. *New Phytologist*, 181, 53–61. Available from: <https://doi.org/10.1111/j.1469-8137.2008.02644.x>
- Zheng, W., Rang, L. & Bergman, B. 2008. Structural Characteristics of the Cyanobacterium–*Azolla* Symbioses. 235–263. Available from: https://doi.org/10.1007/7171_2008_120
- Zheng, W., Rasmussen, U., Zheng, S., Bao, X., Chen, B., Gao, Y. et al. (2013) Multiple modes of cell death discovered in a prokaryotic (Cyanobacterial) endosymbiont. *PLoS One*, 8, e66147. Available from: <https://doi.org/10.1371/journal.pone.0066147>
- Zhu, L., Pietiäinen, M., Kontturi, J., Turkkelin, A., Elomaa, P. & Teeri, T.H. (2022) Polyketide reductases in defense-related parasorboside biosynthesis in *Gerbera hybrida* share processing strategies with microbial polyketide synthase systems. *New Phytologist*, 236, 296–308. Available from: <https://doi.org/10.1111/nph.18328>

SUPPORTING INFORMATION

Additional supporting information can be found online in the Supporting Information section at the end of this article.

How to cite this article: Güngör, E., Savary, J., Adema, K., Dijkhuizen, L. W., Keilwagen, J., Himmelbach, A. et al. (2024) The crane fly glycosylated triketide δ -lactone cornicinine elicits akinete differentiation of the cyanobiont in aquatic *Azolla* fern symbioses. *Plant, Cell & Environment*, 47, 2675–2692. <https://doi.org/10.1111/pce.14907>